Detecting Jumps from Lévy Jump Diffusion Processes

Suzanne S. Lee and Jan Hannig [*]

Abstract

Recent asset-pricing models incorporate jump risk through Lévy processes in addition to diffusive risk. This paper studies how to detect stochastic arrivals of small and big Lévy jumps with new nonparametric tests. The tests allow for robust analysis of their separate characteristics and facilitate better estimation of return dynamics. Empirical evidence of both small and big jumps based on these tests suggests that models for individual equities and overall market indices require incorporating Lévy-type jumps. The evidence of small jumps also helps explain why jumps in the market index are uncorrelated with jumps in its component equities.

JEL classification: G12, C12, C14

Key words: Lévy jumps, nonparametric tests, belief measure, false detection, high-frequency data

1. Introduction

Evidence of stochastic skewness and kurtosis of asset return distributions is well known. A large stream of literature has been devoted to developing better models to incorporate these dynamics and studying their important implications for financial management. Examples include models with stochastic volatility and jumps for derivative pricing, bond pricing, and risk management.[1] This literature is expanding with more advanced continuous-time models using general Lévy jump processes. These models nest most of the existing asset-pricing models and turn out to be flexible in explaining various types of jump risk structures, especially small-jump dynamics that can be described by neither stochastic volatility nor rare Poisson-type jumps. Not only can they accommodate such returns but they also provide pricing formulas as tractable as other, simpler models. Accordingly, their extensive applications have appeared in recent studies such as Carr and Madan (1998), Carr and Wu (2003, 2004, 2007), Huang and Wu (2004), and Bakshi, Carr, and Wu (2008).

In light of this fast-growing literature and subsequent efforts in developing better inference methods (see, e.g., Aït-Sahalia, 2004), we are motivated to distinguish the presence and dynamics of different types of Lévy jump arrivals. As in Aït-Sahalia (2004), we categorize Lévy jumps into Poisson-type as big jumps and the other type as small jumps. In principle, big jumps are changes in asset prices that are rare and much larger than what can be explainable by a diffusion process. These jumps can be detected by applying tests that look for large returns. Recognizing jumps in discrete observations from continuous-time models becomes more difficult if the jump sizes are smaller, because they are of a size that could be in principle attributed to a diffusion process,

---

[1] See Merton (1976), Bakshi, Cao, and Chen (1997), Andersen, Benzoni, and Lund (2002), Duffie, Pan, and Singleton (2000), Aït-Sahalia (2002), Chernov, Gallant, Ghysels, and Tauchen (2003), Johannes (2004), Piazzesi (2003), and Pan (2002).

which makes their direct detection impossible. However, we introduce a new, indirect way to identify their stochastic patterns and show when those jumps should not be simply neglected. We use the intuition that small jumps can be revealed by the fact that returns of a particular size appear with higher frequency than would be expected from a diffusion process.

The ability to detect small jumps is important, first because it provides a robust solution to determine whether incorporating Lévy jumps is ever necessary, as opposed to using a Poisson jump-diffusion process in setting up pricing models for a certain asset class. Second, different jump sizes have different implications for investors depending on their levels of risk aversion. Because our test is designed to detect when these different types of jumps arrive and their size distributions, a better understanding of their separate dynamics and systematic patterns can be achieved, which is expected to be helpful for various financial applications such as market timing, risk management, and asset pricing.

We construct our nonparametric jump test statistics for finding realized returns that are unusual relative to volatility levels estimated based on a consistent estimator for instantaneous volatility in the presence of Lévy jumps. For big jump arrivals, we suggest a detection rule determined from the asymptotic null distribution of the maximums of our test statistic, according to an extreme-value theory. For smaller jump arrivals, we first suggest assessing any presence of Lévy jumps by what we call our QQ test, which is designed to compare realized test statistics with synthetic data generated from the asymptotic null distribution of our test statistic. Once we observe an unusual pattern in the QQ test, we propose using a belief measure constructed to allow us to compute how likely it is that a particular return is due to the jump part of the model. This gives us a threshold to detect arrivals of jumps smaller than big jumps. The application of these two rules allows the decomposition of jump risk, which makes their separate inference possible.

2

We also study how our jump test reacts to arrivals of jumps in the continuous limit and prove that the likelihood of failing to detect any kind of Lévy jumps becomes negligible as we increase the frequency of observations. Therefore, one can detect all sorts of jumps more precisely with observations sampled at higher frequency.

In finite samples, big and small jumps detectable by our rules are frequency-specific. We specify the detectable big and small jumps as a function of data frequency and explain how we can detect them. Simulation studies support our contention that our test can distinguish most Lévy jumps as we increase the frequency of observations. We assume in this study that we have high-frequency observations. As long as high-frequency data are available, our methods can be applied to all sorts of financial time series including individual stocks, indices, interest rates, volatility, exchange rates, or other types of security prices.

There are other estimation methods available for this type of model. These use information from either time-series asset return data or cross-sectional option price data. There are more parametric approaches available such as Fast Fourier transform (FFT), calibration, maximum likelihood, and Bayesian Markov Chain Monte Carlo methods.[2] As is well known, the empirical results based on parametric methods crucially depend on how the analyst specifies the models. In general, nonparametric methods provide robust empirical evidence that is not sensitive to model specification. There are a few nonparametric approaches proposed for dealing with similar issues, such as detecting Lévy jumps, estimating volatility, or estimating jump activity when

---

[2]Carr, Geman, Madan, and Yor (2002) employ Fast Fourier transform (FFT) to convert the characteristic function into a density function and match actual realized return data numerically using fine grids. Carr and Wu (2003) and Huang and Wu (2004) apply a calibration approach to minimize pricing errors in option data, and Carr and Wu (2004) apply maximum likelihood methods in the Kalman filter state-space framework. The reverse question of distinguishing diffusion from jumps is studied by Aït-Sahalia (2004) with a maximum likelihood approach. Li, Wells, and Yu (2008) use a Bayesian approach.

there are Lévy jumps in continuous-time asset pricing models (see Aït-Sahalia and Jacod, 2008, 2009a, 2009b; Barndorff-Nielsen, Shephard, and Winkel, 2006; Mancini, 2006; and Todorov and Tauchen, 2008). We discuss the differences and provide simulation evidence of our test's superior finite-sample performance relative to a comparable test.

Finally, using our new tests, we perform empirical analysis on the overall U.S. market indices and individual equities for five years from January 1, 2002 to December 31, 2006. We find evidence of both small and big jumps in their prices. Specifically, our QQ tests, along with our belief measures, reveal that more Lévy jump arrivals are found in individual equities (on average 0.78%) than in the indices (on average 0.50%). We also find more Poisson-type big jumps in equities (on average 0.41%) than in the indices (on average 0.32%). This evidence of the dynamic arrivals of small jumps in addition to big jumps suggests that the popular stochastic-volatility models with Poisson-type jump models widely used in pricing assets such as derivative securities are likely to miss some important intermediate movements in return dynamics. This evidence also offers a resolution to the puzzle noted in Bollerslev, Law, and Tauchen (2008), that is, why jumps detected in the index are uncorrelated with jumps detected in its component stocks since the index can only jump when there is at least one jump in its component stocks. Existing jump tests tend to miss these small jumps, and we interpret these to be the ones that make up the jumps in the index.

The rest of the paper is organized as follows. Section 2 sets up a theoretical framework for detecting jumps from Lévy jump-diffusion processes and introduces the test. Section 3 discusses the jump detection rules and the asymptotic behavior of the test statistics. Section 4 investigates the test's finite-sample performance by simulation. Empirical evidence found in U.S. equity markets is presented in Section 5. Finally, we conclude in Section 6.

2. A theoretical model for the Lévy jump test

We fix a complete probability space $(\Omega, \mathcal{F}_t, \mathcal{P})$, where Ω is a set of events in a financial market, $\{\mathcal{F}_t\}$ is market information filtration over a time horizon $[0, T]$, and $\mathcal{P}$ is a data-generating measure. This describes financial market uncertainty. We denote $S(t)$ as the asset price at t under $\mathcal{P}$ and write its continuously compounded return as $d \log S(t)$ for $t \in [0, T]$.

We model asset prices to evolve continuously as a particular Lévy jump-diffusion process that is adapted to information filtration $\mathcal{F}_t$. In general, sample paths of Lévy processes are right-continuous with left limits, and have independent increments. They are used to capture non-normal discontinuous increments with various jump dynamics and structures. Their features are specified by the characteristic function whose exponent satisfies the Lévy-Khintchine formula as in Bertoin (1998), displaying characteristics of the process such as its drift, diffusion, and discontinuous components. The Lévy measure determines simultaneously the pure jump-size distribution and intensity, including how often jumps of certain sizes occur over an interval. A purely discontinuous Lévy process can be either a *finite-activity* jump process, which exhibits a finite number of jumps in any finite interval, or an *infinite-activity* jump process, which exhibits infinitely many jumps in any finite interval.

We are interested in detecting and understanding the dynamics of such Lévy jumps in the asset returns in the following framework. Although a Lévy process itself often encompasses a diffusion component, we set in this paper a pure Lévy jump process to be added to a Brownian motion process to describe their dynamics separately. When there is no jump in the market, the asset price $S(t)$ is represented as

$$d \log S(t) = \mu(t)dt + \sigma(t)dW(t), \tag{1}$$

where $W(t)$ is an $\mathcal{F}_t$-adapted standard Brownian motion. The drift $\mu(t)$ and spot volatility $\sigma(t)$ are

$\mathcal{F}_t$-measurable functions such that the underlying process is a diffusion that has only continuous sample paths. When there are Lévy jumps, $S(t)$ is given by a Lévy jump-diffusion model as

$$d \log S(t) = \mu(t)dt + \sigma(t)dW(t) + dL(t), \tag{2}$$

where $L(t)$ is an $\mathcal{F}_t$-adapted Lévy jump process with a Lévy jump measure ν and independent of $W(t)$. We do not specify drift, diffusion, or jump processes further with any particular measure until the simulation study.

Observation of $S(t)$, or equivalently $\log S(t)$, only occurs at discrete times $0 = t_0 < t_1 < ... < t_n = T$ that span the fixed time interval $[0, T]$. For simplicity, this paper assumes that observation times are equally spaced: $\Delta t = t_i - t_{i-1}$. This simplified assumption can easily be generalized to non-equidistant cases by letting $\max_i |t_i - t_{i-1}| \to 0$. We also impose the following necessary assumption on price processes throughout this paper (mathematical forms of this assumption are provided in the Appendix):

Assumption 1. Properties of drift $\mu(t)$ and diffusion $\sigma(t)$ processes

1. $\mu(t)$ and $\sigma(t)$ are smooth and not changing dramatically over a short time interval.

2. $\mu(t)$ and $\sigma(t)$ can be stochastic and can depend on the price process.

3. $\sigma(t) > 0$ for all $t \in [0, T]$.

We only assume a certain level of smoothness in these two coefficients. This assumption is satisfied for most Itô processes that are used for continuous-time asset-pricing models.[3] We do

---

[3]Examples are the constant drift and diffusion coefficient model as in Merton (1976), the stochastic volatility model in Heston (1993), and its extended versions studied in Bakshi, Ju, and Ou-Yang (2006), which allow nonlinearities in the drift coefficients and more flexible diffusion specifications.

not impose any specific assumptions on dependence between the process driving volatility and the price process. Therefore, they can depend on each other, though they do not have to. This assumption excludes jumps in volatility.[4]

For our analysis using high-frequency data, the drift (of order dt) is mathematically negligible compared to the diffusion (of order $\sqrt{dt}$) and the jump component (of order greater than $\sqrt{dt}$). The drift estimates tend to have higher standard errors so that they cause the precision of variance estimates to decrease if included in variance estimation. Omitting drift in our analysis, i.e., $\mu(t) = 0$, is in fact desirable. Hence, in what follows, we state our results ignoring the drift.

2.1. Definition of the nonparametric Lévy jump test

In this subsection, we address the basic intuition behind our development of the new Lévy jump test statistic. Then, we provide its mathematical definition.

The intuition that gives rise to the formation of our test is similar to that of Lee and Mykland (2008), who study a Poisson-type jump test. We first measure local movement of the return process over a window of fixed size and estimate instantaneous stochastic volatility. The last observation in a window is then compared to the estimated stochastic volatility. By going through tests over time, we distinguish jump arrivals.

The main difference between our Lévy jump test and the Poisson jump test by Lee and Mykland (2008) is the stochastic-volatility estimation in the presence of different types of jumps. When there are infinite-activity Lévy jumps in price processes, which we consider in this paper, the scaled realized bipower variation used for their Poisson jump test is no longer sufficient for

---

[4]Although a study by Duffie, Pan, and Singleton (2000) allows correlated double jumps in volatility and in returns, empirical evidence of jumps in volatility is inconclusive in the literature and depends on the methodologies used. For example, see Chernov, Gallant, Ghysels, and Tauchen (2003) and Eraker, Johannes, and Polson (2003).

us to consistently estimate volatility movements. There are two different consistent estimators proposed for integrated volatility in the presence of Lévy jumps in the literature. One is truncated power variation, which is the power variation based on retaining only small increments. The other is multipower variation, which is the scaled sum of the pth power of q successive absolute returns for any $p > 0$ and any integer $q \geq 1$. Because the infinite-activity jumps are likely to appear in successive returns, and hence multipower variation tends to overestimate instantaneous volatility, we use truncated power variation in the construction of our test (see, e.g., Aït-Sahalia and Jacod, 2009b; Barndorff-Nielsen, Shephard, and Winkel, 2006; Huang and Tauchen, 2005; Mancini, 2006).

We now turn to the theoretical setup for the Lévy jump test statistic. Remember that n is the number of observations over the fixed time horizon $[0, T]$. The distance between two successive observations is $\Delta t = \frac{T}{n}$. Consider a local movement of the process within a window of size $K + 1$. With the first K realized returns in the window just before testing time t_i, the instantaneous volatility is estimated based on the realized truncated power variation. We then take the ratio of the last realized return from time t_{i-1} to t_i in the window to this estimated volatility in order to determine whether there is a jump between t_{i-1} and t_i, as well as its size.[5] The mathematical notations are as follows.

Definition 1. The piecewise constant process $\mathcal{T}(t)$, which will be used to test whether there was

---

[5]In our setup, if one is concerned about the presence of jumps in volatility, one can use the last K observations in the window after testing time t_i to estimate the instantaneous volatility and take the ratio of the first realized return in the window to this estimated volatility to form a test statistic. This statistic is valid in the presence of jumps in volatility because the volatility processes are right-continuous with or without jumps. All the theoretical results presented in the following section are also valid with this alternative definition.

a Lévy jump from t_{i-1} to t_i, is defined for $t \in (t_{i-1}, t_i]$ as

$$\mathcal{T}(t) \equiv \frac{\log S(t_i)/S(t_{i-1})}{\widehat{\sigma(t_i)} \, \Delta t^{1/2}}, \quad t \in (t_{i-1}, t_i] \tag{3}$$

where for any $g > 0$, $0 < \widetilde{\omega} < 1/2$, and $t \in (t_{i-1}, t_i]$,

$$\widehat{\sigma(t)}^2 \equiv \frac{\Delta t^{-1}}{K} \sum_{j=i-K}^{i-1} \left(\log S(t_{j-m+1})/S(t_{j-m}) \right)^2 I_{\{|\log S(t_{j-m+1})/S(t_{j-m})| \leq g \Delta t^{\widetilde{\omega}}\}}. \tag{4}$$

Notice that the realized truncated power variation is in the denominator of the statistic, which makes our technique robust to the presence of jumps. We only use $K+1$ (window size) observations included in the local window. We discuss how to choose K in Section 3.1.

3. Asymptotic theory of inference

This section explains the theories behind our proposed tests and discusses how we recognize big and small Lévy jump arrivals. Assuming that model (2) is true, we first prove that it is legitimate to estimate the instantaneous volatility $\sigma(t)$ as in Eq. (4) at any time and use it for our jump test. Next, we describe the limiting behavior of our test statistic and explain how one can detect big jump arrivals using an extreme value theory. Then, we explain what we call our QQ test, which is designed to assess any presence of Lévy jumps, and we introduce our belief measure to detect small jump arrivals. We also prove that when Lévy jumps are present, we can detect Lévy jumps with probability approaching 1, as we increase the frequency of observations.

3.1. Instantaneous volatility estimation

Proposition 1 below shows why the usage of the realized truncated power variation is valid for the instantaneous volatility estimation in the denominator of the test statistic.

Proposition 1. *Let $\widehat{\sigma(t)}$ be as in Eq. (4), $K \to \infty$, and $\Delta t K \to 0$. Suppose the asset return process follows (2), and* **Assumption 1** *is satisfied. Then, as $\Delta t \to 0$,*

$$\widehat{\sigma(\tau)} \xrightarrow{P} \sigma_\tau \tag{5}$$

for any stopping time $\tau > 0$ independent of the process $S(t)$.

The proof of this proposition is in the Appendix. It establishes a pointwise convergence in (5), stating that as long as we use frequent-enough observations and choose the window size properly, instantaneous volatility can be consistently estimated at any time. In order to retain the benefit of the truncated power variation, the window size $K + 1$ must be large enough but smaller than the number of observations n, so that the effect of Lévy jumps in the window on estimating instantaneous volatility disappears, and hence only the volatility level will be extracted. In finite samples, we find from our simulation study that too-large window sizes increase the computational burden without much improvement in the precision of estimation. One way to choose a window size is to find an optimal $K = \widetilde{b} \Delta t^{\widetilde{c}}$, with $-1 < \widetilde{c} < 0$ for some constant $\widetilde{b}$. We use this approach for our analysis.

3.2. Recognizing arrivals of big Lévy jumps

We now study how the jump test process $\mathcal{T}(t)$ interacts with the arrival of Lévy jumps and how to detect big jump arrivals. To investigate the interaction, we suppose that the realized return now follows the Lévy jump-diffusion model as in Eq. (2). Here, it is important to notice that jumps are countable, even if there can be an infinite number of jumps within a finite interval. Hence, there are time points when there is no jump. We prove that the test process remains bounded in probability at those times without a jump: more precisely, when there is no jump in between two

countable observation times. In particular, the test statistic at those times follows approximately a normal distribution in the limit. On the other hand, at the times of jump arrivals, it grows to infinity as Δt goes to 0. Therefore, in theory, we can detect the arrival times of Lévy jumps eventually. Theorem 1 below formally describes the limiting behavior of our test statistic. The proof is relegated to the Appendix.

Theorem 1. *Let $\mathcal{T}(t)$ be as in **Definition 1** and $K \to \infty$ and $\Delta t K \to 0$. Suppose the process follows (2) and **Assumption 1** is satisfied.*

A. For any stopping time τ, such that $\Delta S(\tau) = 0$ almost surely (i.e., there is no jump at time τ almost surely), as $\Delta t \to 0$,

$$\mathcal{T}(\tau) \xrightarrow{\mathcal{D}} N(0,1), \tag{6}$$

where $N(0,1)$ denotes a standard normal random variable.

B. Define the time of the kth jump bigger than h by

$$\tau_{k,h} = \inf\{t > \tau_{k-1,h}, \Delta L(t) > h\}. \tag{7}$$

Then, as $\Delta t \to 0$,

$$P\left(\min_k \frac{\mathcal{T}(\tau_{k,h})}{h/(\sigma(\tau_{k,h})\sqrt{\Delta t})} \geq 1\right) \to 1. \tag{8}$$

Therefore, $\mathcal{T}(\tau_{h,k}) \to \infty$, as $\Delta t \to 0$.

Here, one can test for the presence and arrivals of big jumps by the following rule. To come up with the big-jump test, we hypothesize that our realized returns come from model (1) and we consider how large the magnitude of $\mathcal{T}(t)$ can be by studying the asymptotic null distribution of its maximums in the following proposition. This offers the big-jump detection region. This idea

11

was also used in Lee and Mykland (2008) and we can apply the same in our case for Poisson-type big jumps. The following proposition is taken directly from Lee and Mykland (2008) and we state it for the convenience of readers as well as for our further discussion.

Proposition 2. Big Lévy jump-detection rule

Let $\mathcal{T}(t)$ be as in **Definition 1** *and $K \to \infty$ and $\Delta t K \to 0$. Suppose the process follows (1) and* **Assumption 1** *is satisfied. Then, as $\Delta t \to 0$,*

$$\frac{\max_{t\in(t_{i-1},t_i]} \text{ for } 0\leq i\leq n |\mathcal{T}(t)| - C_n}{S_n} \to \xi, \tag{9}$$

where ξ has a cumulative distribution function $P(\xi \leq x) = \exp(-e^{-x})$,

$$C_n = (2\log n)^{1/2} - \frac{\log \pi + \log(\log n)}{2(2\log n)^{1/2}} \text{ and } S_n = \frac{1}{(2\log n)^{1/2}}. \tag{10}$$

Notice that the test $\mathcal{T}(t)$ is defined as a piecewise constant and the maximum in Eq. (9) is the same as if it were taken at all observation times t_i. The main use of Proposition 2 is to set up the big-jump rejection regions of our test: namely, we detect a big jump arrival at testing time t_i if the absolute value of the test statistic is bigger than $q_{\tilde{\alpha}} S_n + C_n$, where $q_{\tilde{\alpha}}$ is the $\tilde{\alpha}$ quantile of the limiting distribution of maximum ξ.

Combining the results of Proposition 2 and the results of Theorem 1, we see that any jump of a fixed size will be detected by our procedure and see how we categorize big jumps. Specifically, Theorem 1, Part B states that at the time of a jump of size h, the test statistic grows at least as fast as $h/(\sigma(\tau_{k,h})\sqrt{\Delta t})$, which is of the order of $\Delta t^{-1/2} = n^{1/2}$. On the other side, for the significance level $\tilde{\alpha}$, remember that the big-jump detection cutoff for our test is set in Proposition 2 as $q_{\tilde{\alpha}} S_n + C_n$, which is of the order of $\sqrt{\log(n)} = \sqrt{-\log(\Delta t)}$. An immediate consequence of these

facts is that as Δt decreases, we are able to detect smaller and smaller jumps. In particular, we should be able to detect all jumps of size h_n, where $h_n / \sqrt{-2\max(\sigma(t))\Delta t \log(\Delta t)} \to \infty$. In other words, we expect to detect jumps of a size larger than $\sqrt{-2\max(\sigma(t))\Delta t \log(\Delta t)}$, and we will not be able to detect jumps of a size smaller than $\sqrt{-2\max(\sigma(t))\Delta t \log(\Delta t)}$ with our big-jump detection rule. Notice that this threshold $\sqrt{-2\max(\sigma(t))\Delta t \log(\Delta t)}$ converges to zero as $\Delta t \to 0$. Therefore, we can detect more jumps as we increase the frequency of observations.

3.3. Assessing Lévy jumps: QQ test and multiple test adjustment

The big-jump test described in Section 3.2 will detect jumps that are much larger in size than the natural variation of the diffusion process. In this subsection, we describe a test that can detect the presence of Lévy jumps that are smaller than jumps detectable by our big-jump test. Instead of looking for unusually large returns as our big-jump test does, it looks for returns that occur with unusual frequency. In particular, the test marks the presence of Lévy jumps if it finds the number of test statistics of a particular size to be significantly different from what would have been expected under the no-jump model. In other words, it looks for an over or underabundance of test statistics across all possible values through a multiple test. The test can, therefore, sense rather small jumps provided they are prevalent enough. We call this the QQ test in this paper.

To be more specific, suppose we have a time horizon $[0, T]$ over which we are interested in finding the presence of Lévy jumps. Every time we have a realized return within the time horizon, we can perform a single test at a particular time using the following asymptotic distribution of our test statistic. This proposition can be also deduced from Theorem 1, Part A. We state it along with related properties for our further discussion.

Proposition 3. *Let $\mathcal{T}(t)$ be as in **Definition 1** and $K \to \infty$ and $\Delta t K \to 0$. Suppose the process follows (1) and **Assumption 1** is satisfied. Then, as $\Delta t \to 0$,*

$$\mathcal{T}(t) \xrightarrow{\mathcal{D}} N(0,1), \tag{11}$$

where $N(0,1)$ denotes a standard normal random variable, and hence, as $\Delta t \to 0$,

$$\Phi(\mathcal{T}(t)) \xrightarrow{\mathcal{D}} U(0,1), \tag{12}$$

where $\Phi(z)$ is the cumulative distribution function (CDF) of standard normal variable z and $U(0,1)$ denotes a uniform random variable.

Proposition 3 is the basis for our multiple test. This result suggests comparing the distribution of our observed test statistics computed from realized asset returns with standard normal distribution using the QQ-plot (a QQ-plot is a simple diagnostic tool for identifying differences in distributions (such as non-normality) from which data have been taken). If there is no jump present, the distribution of the test statistics $\{\mathcal{T}(t_{K+1}), \mathcal{T}(t_{K+2}), \ldots, \mathcal{T}(t_n)\}$ in theory would converge to an i.i.d. standard normal as $n \to \infty$. Hence, a QQ-plot of the standard normal quantiles versus the quantiles of the test statistics should also converge to a 45-degree line in the limit.

However, because of random variability and discreteness as well as the stochastic volatility estimation risk, the QQ-plot can deviate from the 45-degree line even if there is no jump. Therefore, we need to assess how much of this deviation is natural under the no-jump model. For this purpose, we apply a procedure based on ideas in Hernandez-Campos, Samorodnitsky, and Smith (2004). Specifically, we investigate the asymptotic null distributions of quantiles as follows.

First, remember that we had n observations and that the first K observations are used for volatility estimation. Hence, we have $n-K$ test statistics, normally distributed under the no-jump

model. We simulate m independent copies of a data set containing $n - K$ i.i.d. standard normal variables. For each of the m data sets, we plot the QQ-plots with dot-dashed lines. These m QQ-plots create an envelope that shows the natural deviation of the QQ-plot from the 45-degree line under the no-jump model. This gives us the asymptotic null distributions of quantiles. If the QQ-plot of the data leaves the envelope, i.e., if any realized quantile lies beyond its generated null distribution, we conclude that there is a significant departure from the no-jump model.

The number of synthetic datasets m used to create the envelope controls the statistical significance level of our multiple tests. Under the null, a simple calculation reveals that the probability that a particular test value lies outside the envelope is $2/(m+1)$. However, since the data consists of a large number $(n - K)$ of test statistic values, we need to do a multiple testing adjustment to control the overall significance level $\tilde{\alpha}$ of our test. For example, one could apply the Bonferroni adjustment leading to $m = (n - K)/\tilde{\alpha} - 1$. However, Bonferroni adjustment is known to be overly conservative and we do not recommend its use in practice. Instead, we suggest adjustment based on simulation of the extremes of the normal QQ-plots.

The approach used to find m is as follows. When there is no jump at any time during the entire time horizon, test statistics will be approximately normally distributed as stated in Proposition 3. We first apply the true distribution function (standard normal CDF) of the test statistic to both the test statistic and the envelope. We know that all the statistics and envelopes transformed according to the distribution function follow a uniform distribution, as stated in Proposition 3. Now, notice that the probability that the transformed test statistic trace stays inside the envelope becomes

$$P \left(\min_{j=1,\ldots,m} U_{(k),j} \leq U_{(k)} \leq \max_{j=1,\ldots,m} U_{(k),j}, k = 1, \ldots, n - K \right), \tag{13}$$

where $U_{(k)}$ represent the transformed test statistic values. They are the order statistics based on

i.i.d. U(0,1) random variables U_l, $l = 1, \ldots, n - K$. Similarly, the $U_{(k),j}$ represent the transformed envelope. They are the order statistics based on i.i.d. U(0,1) random variables $U_{i,j}$, $i = 1, \ldots, n - K$ independent of U_l.

For any fixed $n - K$ and desired overall significance level $\tilde{\alpha}$, we then find m for which the probability in (13) comes as close to $1 - \tilde{\alpha}$ as possible. These m can be simply found by simulation, and the recommended values of m for various numbers of statistics $n - K$ and significance levels $\tilde{\alpha}$ are listed in Table 1. As seen in the table, given the number of available observations, we require a greater m for a lower overall significance level. And for a fixed significance level, as we have more observations, a greater m would be required.

3.4. Recognizing arrivals of small Lévy jumps

As noted in Section 3.3, the presence of jumps that are not detectable by our big-jump rule can still be assessed by our QQ test, since the QQ test is more sensitive to the presence of Lévy jumps than the big-jump test. Provided that we assess their presence using the QQ test, we still would like to be able to distinguish arrivals of these small jumps to determine which returns are due to the jump part. In the case of the big-jump detection rule, the flagged test statistics are so large that it is virtually certain they are the result of a jump. In the case of the QQ test, we only detect a significant overrepresentation of a particular value of a test statistic that could also be present just through normal fluctuation from the no-jump model. Therefore, it is possible that some of the returns flagged by the QQ test are due to jumps while others are not. In other words, there can be false arrival detections if we use only the QQ test. In order to control such false detections, we propose a way to measure the belief or likelihood that a particular realized return at a testing time is not due to normal random fluctuation from the diffusion model.

We now proceed to define a belief measure to control false detection. Here, we need some

16

Table 1: **Number of synthetic datasets m needed for the QQ test**[†]

$n-K$	$\tilde{\alpha}=1\%$	$\tilde{\alpha}=5\%$	$\tilde{\alpha}=10\%$	$n-K$	$\tilde{\alpha}=1\%$	$\tilde{\alpha}=5\%$	$\tilde{\alpha}=10\%$
78	5,503	932	422	96	6,089	1,044	456
100	6,211	1,063	463	130	7,057	1,189	510
250	9,204	1,513	649	260	9,334	1,533	658
288	9,668	1,584	683	390	10,716	1,744	753
480	11,498	1,864	803	500	11,658	1,888	813
520	11,815	1,912	823	780	13,557	2,158	930
960	14,451	2,288	988	1,000	14,618	2,314	1,000
1,440	15,859	2,562	1,111	1,560	16,112	2,620	1,137
1,920	16,789	2,775	1,203	1,950	16,841	2,787	1,208
2,500	17,691	2,956	1,280	2,880	18,194	3,040	1,318
3,900	19,320	3,217	1,403	4,680	20,031	3,329	1,457
5,000	20,295	3,371	1,477	5,760	20,873	3,461	1,521
7,200	21,816	3,609	1,593	7,800	22,165	3,663	1,618
10,000	23,284	3,838	1,689	14,400	25,028	4,109	1,793
15,600	25,429	4,171	1,816	17,280	25,949	4,251	1,846
23,400	27,556	4,500	1,940	25,000	27,920	4,556	1,961
28,800	28,714	4,678	2,006	31,200	29,173	4,749	2,033
46,800	31,613	5,123	2,171	50,000	32,030	5,187	2,194
57,600	32,941	5,326	2,245	86,400	35,697	5,746	2,398
93,600	36,268	5,833	2,430	100,000	36,747	5,906	2,452
115,200	37,791	6,064	2,483	117,000	37,908	6,082	2,485
172,800	40,953	6,543	2,521	234,000	43,489	6,925	2,524
345,600	46,983	7,449	2,524	432,000	49,107	7,767	2,524

[†] Number of synthetic datasets m needed to obtain a desired overall significance $\tilde{\alpha}$ for the multiple test, when we have $n-K$ multiple tests. The values in this table were simulated and smoothed using a monotone quadratic regression spline.

notation. Recall that (3) effectively defines n different test statistics and encodes them in the test statistic process $\mathcal{T}(t_i)$. The first K test statistics are not well defined because our volatility estimator needs the first K observations. Hence, we take the remaining $n - K$ test statistics, order them as in the following Definition 2, and use them as a basis of our test.

Definition 2. Let the ordering function $r(i)$ be defined to satisfy $\mathcal{T}(t_i) = T_{(r(i))}$ for all $i = K+1, .., n$, where the observed test statistics are $\{\mathcal{T}(t_{K+1}), \mathcal{T}(t_{K+2}), \ldots, \mathcal{T}(t_n)\}$ and their order statistics are $\{T_{(1)}, \ldots, T_{(n-K)}\}$, so that $\{T_{(1)} \leq .. \leq T_{(n-K)}\}$.

Notice that each of the intervals $((T_{(r-1)} + T_{(r)})/2, (T_{(r)} + T_{(r+1)})/2)$ contains exactly one value of the test statistic, that is $T_{(r)}$. We now show that under the no-jump model, the expected number of test statistics in this interval is also about one. Recall that Proposition 3 implies that the $\mathcal{T}(t_i)$ are asymptotically independent normal random variables under the no-jump model. The following proposition gives us guidance in setting up our belief measure.

Proposition 4. *Let* $T_{(1)}, \ldots, T_{(N)}$ *be the order statistics computed as in* **Definition 2** *from a sample of* N *independent standard normal random variables. Then, the random variable* $\mathcal{B}_r = \Phi((T_{(r)} + T_{(r+1)})/2) - \Phi((T_{(r-1)} + T_{(r)})/2)$ *have* $Beta(2, N-1)/2$ *distribution. Furthermore, its expected value is* $E\mathcal{B}_r = 1/(N+1)$ *and the covariance is*

$$
\mathrm{Cov}(\mathcal{B}_r, \mathcal{B}_l) = \begin{cases} \frac{N-1}{2(N+2)(N+1)^2} & \text{if } r = l, \\[2mm] \frac{N-3}{4(N+2)(N+1)^2} & \text{if } |r - l| = 1, \\[2mm] -\frac{1}{(N+2)(N+1)^2} & \text{if } |r - l| > 1. \end{cases}
$$

The proposition is proved using simple algebra. We omit the details to save space. This proposition suggests using the following test statistic as a first step toward defining our belief measure:

$$\tilde{l}(r) = 1 - (n - K + 1)\left(\Phi((T_{(r)} + T_{(r+1)})/2) - \Phi((T_{(r-1)} + T_{(r)})/2)\right),$$

where $r = 1, .., n - K$. Here, the first term, 1, is the number of test statistics in the interval $((T_{(r-1)} + T_{(r)})/2, (T_{(r)} + T_{(r+1)})/2)$, while $(n - K + 1)\Phi((T_{(r)} + T_{(r+1)})/2) - \Phi((T_{(r-1)} + T_{(r)})/2)$ approximates the expected number of test statistics observed in the same interval under the no-jump model, according to the first part of Proposition 4. Now, if we have a significant over-representation of test statistics of a certain size, the spacings in between them would be shorter than expected, leading to a smaller expected number of test statistics in the interval than that under the null. The value of $\tilde{l}(r)$ then becomes closer to one, indicating that this particular test statistic is more likely due to a jump.

However, Proposition 4 also states that, even though the expectation of $\tilde{l}(r)$ under the no-jump model is close to zero, the variance of $\tilde{l}(r)$ remains bounded away from zero. Therefore, the raw values of $\tilde{l}(r)$ are not by themselves reliable measures of belief. To solve this problem, we assume that the likelihood of a test statistic being the result of a jump is continuous as a function of its size, which means that belief measures should be close if the values of the test statistics are close. Thus, we suggest obtaining a smoothed measure $l(r)$ by locally averaging the values of $\tilde{l}(r)$ for values of $T_{(r)}$ close to each other. In particular, we propose using the Nadaraya-Watson estimator to do this smoothing. To use this estimator in practice, one of the parameters that needs to be selected is the window-width. Window-width could be understood as the amount of averaging to get our smoothed value $l(r)$. The choice of window-width has been intensively studied in the statistical literature. We have decided to use an automatic choice of window-width

proposed by Ruppert, Sheather, and Wand (1995) called the DPI method. It follows from the theory of smoothing, wherein under the no-jump model, $l(r) \xrightarrow{P} 0$. Interested readers can consult Fan and Gijbels (1996) for more details.

This leads us to define the belief measure for a return at t_i as

$$b(t_i) = \max(0, l(r(i)),$$

where $r(i)$ is the ordering function as in Definition 2 and $l(r(i))$ is the smoothed value as described above. We use $b(t_i)$ as a measure of the belief that a particular return is the result of a jump. In particular, with a chosen false detection rate of $\hat{\alpha}$, it guarantees that among returns of likelihood $b(t_i) \geq (1 - \hat{\alpha})$, we would expect to have at least $(1 - \hat{\alpha}) \times 100\%$ of returns that are due to jumps and at most $\hat{\alpha} \times 100\%$ of returns that are due to random fluctuations of the no-jump model. Notice that we use this belief measure only after the QQ test rejects the no-jump model.

Finally, we summarize the use of our small-jump tests as follows. First, select the number of traces m from Table 1 for creating the envelope in the QQ test according to the number of tests and desired significance level $\tilde{\alpha}$. Then, check if the QQ-plot based on realized test statistics leaves the envelope. If it does not, conclude that there is not enough evidence to reject the diffusion model. If the QQ-plot of realized test statistics does leave the envelope, we have enough evidence to prove the presence of Lévy jumps. To locate actual arrivals of jumps, compute the belief measure $b(t_i)$. Then, select a desired false detection rate $\hat{\alpha}$. Note that it is possible that $\tilde{\alpha} \neq \hat{\alpha}$. Flag as Lévy jumps all returns with $b(t_i) \geq (1 - \hat{\alpha})$. It is important to bear in mind that among the flagged returns there could be as many as $\hat{\alpha} \times 100\%$ false positives. This belief measure converges to one as we have bigger jump sizes, because the value of the test statistics converges to infinity in such cases. To determine if Poisson jump-diffusion models are not sufficient to describe any asset return dynamics, we can compare the results from our big-jump test with those from this

small-jump test. If we find considerably more jumps from the latter test than from the big-jump test, we can conclude that Lévy jumps are significant. Furthermore, to decompose Lévy jump risk into big and small jumps, we can apply this approach along with big-jump detection rule and categorize as big jumps those detected by our big-jump rule and as small jumps those not detected by our big-jump rule but detected by our belief measure.[6]

4. Monte Carlo Simulation

In this section, we examine the finite-sample performance of our Lévy jump test using Monte Carlo simulation. Our asymptotic argument requires continuous sampling, which cannot be perfectly met in real applications. Through simulation, we show that high-frequency data allow us to achieve better inference results. We also compare the results of our test to another comparable existing Lévy jump test and present our superior performance. For all series generation, we use the Euler-Maruyama stochastic differential equation (SDE) discretization scheme (Kloeden and Platen, 1992), an explicit order 0.5 strong and order 1.0 weak scheme. We discard the burn-in period—the first part of the whole series—to avoid the starting value effect, every time we generate each series. For all cases in this section, we simulate returns at various frequencies such as one minute, 15 seconds, or 5 seconds over one trading day, assuming 6.5 trading hours per day. We choose to consider the horizon of one day ($T = \frac{1}{252}$) as a typically relevant time length in trading, hedging, and other applications.

The infinite-activity jump model we consider for simulation is the Lévy α-stable process. Jump sizes from this process follow an α-stable distribution, denoted as $S_\alpha(\beta, \delta, \gamma)$, with a tail

---

[6] An estimate of the number of jumps detected in a fixed time interval (without the need to know their exact location) can be obtained by adding up the values of the belief measure for returns over that interval. This approach is used in calculating the estimate of the detected small jump intensity presented in Figs. 4 and 7.

index $\alpha \in (0, 2]$ for the shape of the size distribution, a skew parameter β for the skewness of distribution, a scale parameter $\delta \geq 0$, and a location parameter γ. In our analysis, we choose to study the performance of our test on jumps from the finite moment log-stable process of Carr and Wu (2003) and Li, Wells, and Yu (2008). According to both studies, we set $\beta = -1$ to achieve negative skewness of empirical densities of equity index returns. We take the characteristic function of the α-stable distribution given by

$$E[exp(iuL(t))] = exp(-\delta^{\alpha}|u|^{\alpha}[1 - i\beta(\tan\frac{\pi\alpha}{2})(\text{sign }u)] + i\gamma u), \alpha \neq 1$$

$$E[exp(iuL(t))] = exp(-\delta|u|[1 + i\beta\frac{2}{\pi}(\text{sign }u)(\log|u|)] + i\gamma u), \alpha = 1.$$

For $\alpha < 1$, the support for stable density is only a positive real line. In order to keep the support of these stable densities on the whole real line, we should only allow $\alpha \in [1, 2]$. The α-stable process reduces to some well-known special cases. If $\alpha = 1, \beta = 0, \delta = 1$, and $\gamma = 0$, it becomes a standard Cauchy process. If $\alpha = 2, \beta = 0, \delta = 1$, and $\gamma = 0$, it becomes a standard Gaussian process. For our simulation study, we use $\alpha = 1.7629$, following Li, Wells, and Yu (2008). (According to our unreported results, the level of α might affect performance but the difference is not significant and our conclusion is not altered, depending on α.) To simulate general stable random variables, we use the algorithm by Chambers, Mallows, and Stuck (1976), which involves a nonlinear transformation of two independent uniform random variables into one stable random variable. Since it produces standard stable variables with mean zero and unit variance, we transform again to obtain our desired series.

We consider both constant and stochastic volatility models. For constant volatility, we set $\sigma(t) = 30\%$ per year, which is usual for U.S. equity markets. For stochastic volatility, we consider a one-factor affine model. We assume the stochastic volatility model as in Heston (1993), specified

as the following square root processes (see Cox, Ingersoll, and Ross, 1985):

$$d\sigma^2(t) = \kappa \left(\bar{\varsigma} - \sigma^2(t)\right) dt + \omega\sigma(t)dB(t), \tag{14}$$

where $B(t)$ denotes a Brownian motion. For $\kappa, \bar{\varsigma}$, and ω, we use the parameter estimates from equity markets reported in the empirical study by Li, Wells, and Yu (2008, Table 4): $\kappa = 0.0162, \bar{\varsigma} = 0.8465$, and $\omega = 0.1170$, to mimic real market returns. For estimation of the truncated power variation, we use parameter values of $g = 1.2$, which is four times the usual volatility $\sigma(t) = 30\%$, and $\widetilde{\omega} = 0.47$, following Aït-Sahalia and Jacod (2009b).

4.1. Constant volatility versus stochastic volatility without Lévy jumps

Before we present the performance of our test in detecting jumps, we first show the size of the test, that is, how often our jump tests falsely detect jump arrivals when there is no jump in returns.

The employed model for simulation is

$$d\log S(t) = \sigma(t)dW(t), \tag{15}$$

where $\sigma(t)$ is volatility and $W(t)$ is a Brownian motion. We apply both big-jump and small-jump tests. The results with the significance level $\tilde{\alpha} = 5\%$ are reported in Table 2. As can be seen in the table, all the probabilities of spuriously detecting jumps when there is no jump are around 5% at all frequencies under consideration. Big-jump tests tend to give lower rates than small-jump tests, which is expected from the levels of the thresholds we suggest using.

4.2. Constant volatility versus stochastic volatility with Lévy jumps

We first study the performance of our big-jump test in the presence of both diffusion and small jumps. In general, Poisson jumps, which we call big jumps in this paper, are a part of the Lévy

Table 2: **Probability of spuriously detecting jumps using the Lévy jump test**[†]

Frequency Δt	Constant volatility		Stochastic volatility	
	Big-jump test	Small-jump test	Big-jump test	Small-jump test
1 minute	0.044	0.048	0.042	0.051
15 seconds	0.050	0.056	0.043	0.055
5 seconds	0.031	0.048	0.046	0.051

[†] This table presents the size of the test, that is, the rate of rejecting the diffusion model when there is no jump using our big-jump and small-jump tests, as discussed in Section 3. The encompassing model is $d \log S(t) = \sigma(t)dW(t)$, where $W(t)$ is a Brownian motion. Constant volatility is set at $\sigma(t) = \sigma = 30\%$. Stochastic volatility assumes the affine model of Heston (1993), specified as $d\sigma^2(t) = \kappa \left(\bar{\varsigma} - \sigma^2(t) \right) dt + \omega \sigma(t) dB(t)$, where $B(t)$ denotes a Brownian motion. The parameter values used for stochastic volatility simulation are the estimates from equity markets reported in the empirical study by Li, Wells, and Yu (2008, Table 4): $\kappa = 0.0162, \bar{\varsigma} = 0.8465$, and $\omega = 0.1170$. The significance level $\tilde{\alpha}$ is 5%. A fixed time horizon of one trading day ($T = \frac{1}{252}$) is considered. The parameter values used for the truncated power variation estimation are $g = 1.2$ and $\tilde{\omega} = 0.47$. The number of simulations used in this study is 1,000.

jumps. For instance, if one selects Lévy jumps that are greater in size than a certain level, those selected become Poisson jumps. However, in order to ensure the presence of big jumps in addition to small jumps and to control their magnitudes, we separately add Poisson jumps and choose their relative sizes in this simulation. Hence, we simulate returns from

$$d \log S(t) = \sigma(t)dW(t) + \theta_{L,S}dL(t) + \theta_{L,B}dP(t), \tag{16}$$

where $dP(t)$ denotes a Poisson jump arrival indicator and the other notations such as $\sigma(t)$, $W(t)$, and $L(t)$ are the same as before. We denote $\theta_{L,S}$ as the small-jump size parameter and $\theta_{L,B}$ as the big-jump size parameter. Table 3 shows the power of the test, which is the big-jump detection rate. We set $\theta_{L,S} = 0.3$ for small jumps and $\theta_{L,B} = 1$ and 3 for big jumps. As can be seen in the table, the test has a decent detection power for big jumps. The table also shows that the levels of $\theta_{L,B}$ or stochastic volatility do not make much difference in detection power. We also find that better performance can be achieved as we increase the frequency of observations.

In addition to the parameter settings reported in Table 3, we perform the same analysis with other values of jump size parameters such as $\theta_{L,S} = 1$ for small jumps and $\theta_{L,B} = 3$ and 10 for big jumps. We find the power of our test to be 1.000 in all frequencies with both constant and stochastic volatility.

Next we examine the performance of the small-jump test defined in Section 3. We again use the detection rates as the performance measure. This time, assuming that the big-jump test has been separately applied and we have already detected big jumps, we simulate returns from the following Lévy jump-diffusion model:

$$d \log S(t) = \sigma(t)dW(t) + \theta_L dL(t), \tag{17}$$

where all the notations $\sigma(t)$, $W(t)$, and $L(t)$ are the same as before. θ_L denotes the jump size parameter. We choose to consider small jumps whose θ_L are 0.15 and 0.3, which make jump sizes relatively small compared to diffusion.

Overall results presented in Table 4 indicate that high-frequency observations help to improve detection power for small jumps. We also find that our test works well under stochastic volatility. Considering the relative sizes of jumps compared to volatility levels, it is important to note that we achieve good detection power for such small Lévy jumps.

We perform the same analysis with the jump size parameter $\theta_L = 1$ and 2. We find the power of our test to be 1.000 in all frequencies with both constant and stochastic volatility.

4.3. Comparison with other Lévy jump test

A test comparable to ours (denoted as LH hereafter) is the test by Aït-Sahalia and Jacod (2009b) (denoted as AJ hereafter) in that both tests employ nonparametric approaches for the presence of

Table 3: **Probability of detecting big Lévy jumps**[†]

	Constant volatility		Stochastic volatility	
Frequency	Big jump size $\theta_{L,B}$ with $\theta_{L,S} = 0.3$			
Δt	$\theta_{L,B} = 1$	$\theta_{L,B} = 3$	$\theta_{L,B} = 1$	$\theta_{L,B} = 3$
1 minute	0.820	0.910	0.846	0.883
15 seconds	0.972	0.986	0.991	0.996
5 seconds	1.000	1.000	1.000	1.000

[†] This table presents the performance of the big-jump detection rule discussed in Section 3.2. The table contains the power of the test, that is, the probability of detecting big Lévy jumps within a fixed time interval of one trading day $(T = \frac{1}{252})$. The encompassing model is $d \log S(t) = \sigma(t)dW(t) + \theta_{L,S}dL(t) + \theta_{L,B}dP(t)$, where $L(t)$ is an α-stable Lévy jump from $S_\alpha(-1, 1, 0)$ with $\alpha = 1.7629$, $P(t)$ is a Poisson jump, and $W(t)$ is a Brownian motion. $\theta_{L,S}$ denotes the small jump size parameter and $\theta_{L,B}$ denotes the big jump size parameter. Although the Lévy jump $dL(t)$ itself includes Poisson jumps, in order to ensure the presence of big jumps in addition to small jumps and to control their magnitudes, we add Poisson jumps and specify the size with $\theta_{L,B}$. Constant volatility is set at $\sigma(t) = \sigma = 30\%$. Stochastic volatility assumes the affine model of Heston (1993), specified as $d\sigma^2(t) = \kappa \left(\bar{\varsigma} - \sigma^2(t) \right) dt + \omega\sigma(t)dB(t)$, where $B(t)$ denotes a Brownian motion. The parameter values used for stochastic volatility simulation are the estimates from equity markets reported in the empirical study by Li, Wells, and Yu (2008, Table 4): $\kappa = 0.0162, \bar{\varsigma} = 0.8465$, and $\omega = 0.1170$. The parameter values used for truncated power variation estimation are $g = 1.2$ and $\widetilde{\omega} = 0.47$. The significance level $\tilde{\alpha}$ is 5%. The number of simulations used in this study is 1,000.

Table 4: **Probability of detecting small Lévy jumps**[†]

Frequency Δt	Constant volatility		Stochastic volatility	
	Small jump size θ_L			
	$\theta_L = 0.15$	$\theta_L = 0.3$	$\theta_L = 0.15$	$\theta_L = 0.3$
1 minute	0.460	0.886	0.510	0.890
15 seconds	0.886	1.000	0.943	1.000
5 seconds	1.000	1.000	1.000	1.000

[†] This table presents the performance of the small-jump test discussed in Section 3.3. The table contains the power of the test, that is, the probability of detecting α-stable Lévy jumps within a fixed time interval of one trading day ($T = \frac{1}{252}$). The encompassing model is $d \log S(t) = \sigma(t)dW(t) + \theta_L dL(t)$, where $L(t)$ is an α-stable Lévy jump from $S_\alpha(-1, 1, 0)$ with $\alpha = 1.7629$ and $W(t)$ is a Brownian motion. We choose θ_L at 0.15 and 0.3, to consider small jumps compared to diffusion, assuming that big jumps have been detected by our big-jump test. Constant volatility is set at $\sigma(t) = \sigma = 30\%$. Stochastic volatility assumes the affine model of Heston (1993), specified as $d\sigma^2(t) = \kappa \left(\bar{\varsigma} - \sigma^2(t) \right) dt + \omega\sigma(t)dB(t)$, where $B(t)$ denotes a Brownian motion. The parameter values used for stochastic volatility simulation are the estimates from equity markets reported in the empirical study by Li, Wells, and Yu (2008, Table 4): $\kappa = 0.0162, \bar{\varsigma} = 0.8465$, and $\omega = 0.1170$. The parameter values used for estimating the truncated power variation are $g = 1.2$ and $\widetilde{\omega} = 0.47$. The significance level $\tilde{\alpha}$ is 5%. The number of simulations used in this study is 1,000.

Lévy jumps. Unlike parametric inference methods, as discussed in the introduction, nonparametric tests are not sensitive to model specification; hence, robust conclusions can be reached by both tests. Both tests (AJ and LH) are based on asymptotic theories and suggest using high-frequency returns for their application. The main difference between the AJ test and ours (LH) is that the AJ test depends on the intuition that the limits of *integrated* volatility estimators, calculated by the sums of absolute $\widetilde{p}$-th powers with $\widetilde{p}$ greater than two, do not depend on observation frequencies when there are jumps. It compares the estimators based on data sampled at two different frequencies, say, one-minute and two-minute returns, over an interval. By contrast, our approach computes a test statistic for each individual observation in the interval and detects whether the empirical distribution of the test statistic is compatible with the theoretical distribution of the test statistic under the no-jump model. This allows us to detect not only the presence of jumps but also their location. Therefore, our test can distinguish the arrival times, directions (signs), and sizes of Lévy jumps within the interval. Both tests rely on asymptotic results by letting the distance between two successive observations approach zero. Neither test takes account of market microstructure noise in its construction.

Here, we compare the finite-sample performance of two test statistics in detecting jumps and provide simulation evidence that our test outperforms the AJ test. For a proper comparison, we choose the AJ test developed under the null hypothesis of no jump because our test is developed under the null hypothesis of no jump. This allows us to set the same significance level in both tests. As a performance measure, we use the power of these two tests, that is, the rate of rejecting the null hypothesis of no jump when there are jumps. Aït-Sahalia and Jacod (2009b) report the level (size) of their test but not the power of the test, which we present. For the AJ test, given a significance level, we specifically apply the rejection rule suggested in Theorem 6 of their paper,

which is based on the asymptotic null distribution of their test statistic. Using this theory-based rejection rule, we first confirm the size of this test and then, apply it in our study on its power. We choose the parameter values of $p = 4$ and $k = 2$ as in their simulation study. Since both tests require truncating returns, we apply the same level of threshold ($g = 1.2$ and $\widetilde{\omega} = 0.47$) by using the same truncation parameters on both tests.

Aït-Sahalia and Jacod (2009b) also have their other test developed under the null hypothesis that jumps are present and report the level (size) of their other test. We cannot compare the performance of our test to this other test because its null hypothesis is different from ours, and setting the same significance levels for tests developed under different null hypotheses does not make sense for comparison.

We apply the two tests on the same series generated by the following stochastic differential equations,

$$d \log S(t) = \sigma dW(t) + \theta_L dL(t).$$

For $L(t)$, we consider both a Cauchy process and an α-stable Lévy jump process. Other notations are as before. In particular, θ_L denotes the jump size parameter. We set θ_L at $1, 2, 3$, and 4 with a constant volatility of $\sigma = 30\%$ to show how their performance varies depending on jump sizes. The number of simulations in this study is 1,000. We consider several frequencies of observations such as one minute, 15 seconds, 5 seconds, and 1 second during 6.5 hours over one trading day ($T = \frac{1}{252}$). A significance level of 5% is used for both tests. The performance for both tests improves as we increase the frequency of observations. Table 5 presents the two rejection rates next to each other for direct comparison. The results of this comparison study show that our test outperforms the AJ test developed under the null hypothesis of no jump in all frequencies and jump sizes.

Table 5: **Comparison of the power of the proposed test (LH) and the Aït-Sahalia and Jacod (2009b) test (AJ)**[†]

Detecting Cauchy jumps								
Frequency				Jump size θ_L				
Δt		1		2		3		4
	AJ	LH	AJ	LH	AJ	LH	AJ	LH
1 minute	0.31	0.54	0.38	0.74	0.41	0.88	0.45	0.93
15 seconds	0.58	0.76	0.75	0.93	0.82	0.97	0.91	0.99
5 seconds	0.73	0.88	0.90	0.98	0.96	0.99	0.98	1.00
1 second	0.87	0.97	0.99	1.00	1.00	1.00	1.00	1.00
Detecting α-stable jumps								
Frequency				Jump size θ_L				
Δt		1		2		3		4
	AJ	LH	AJ	LH	AJ	LH	AJ	LH
1 minute	0.77	0.99	0.78	1.00	0.79	1.00	0.79	1.00
15 seconds	0.96	1.00	0.97	1.00	0.97	1.00	0.98	1.00
5 seconds	0.99	1.00	0.99	1.00	0.99	1.00	0.99	1.00
1 second	1.00	1.00	1.00	1.00	1.00	1.00	1.00	1.00

[†] This table reports the performance of our test and the AJ test, measured by the power of tests, that is, the rate of rejecting the null hypothesis of no Lévy jumps when there are jumps. Return series are simulated from the mixture of Lévy jumps with Brownian motion as $d\log S(t) = \sigma dW(t) + \theta_L dL(t)$, where $L(t)$ is either a Cauchy process or an α-stable process from $S_\alpha(-1, 1, 0)$ with $\alpha = 1.7629$, and $W(t)$ is a Brownian motion process. Constant volatility is set at $\sigma = 30\%$. We assume 6.5 trading hours per day and the time horizon is set at one trading day ($T = \frac{1}{252}$). The jump size parameter θ_L is selected at 1, 2, 3, and 4. The parameter values used for estimating truncated power variations are $g = 1.2$ and $\widetilde{\omega} = 0.47$. The significance level to detect jump arrivals is 5%. The rates reported in AJ columns are based on their standardized test according to the asymptotic theory described in Aït-Sahalia and Jacod (2009b,Theorem 6). The number of simulations used in this study is 1,000.

5. Empirical analysis for U.S. equity markets

In this section, we apply our new Lévy jump tests to investigate the presence and dynamics of Lévy jumps in the U.S. overall market and individual equity markets. In particular, we study how our new tests detect big and small jump arrivals.

5.1. Data

We collect transaction data for U.S. market indices and individual stocks from the Trade and Quote (TAQ) database. We choose two main indices, the S&P 500 and the Dow Jones Industrial Average, as well as individual equities included in the Dow Jones Industrial Average. We choose transactions on the New York Stock Exchange (NYSE). Our sample period is five years from January 1, 2002 to December 31, 2006. Over this five year time horizon, we calculate five minute returns by taking the first differences of log transaction prices. We select five minutes as our frequency of observations because given the time horizon of five years, it is frequent enough for our jump tests to achieve sufficient power and, as noted in Andersen, Bollerslev, Diebold, and Ebens (2001), market microstructure effects such as bid-ask bounce can be mitigated with data of five-minute frequency or less.

We also pre-process the raw data to avoid unnecessary data-recording errors. We exclude all recording errors such as zero prices. As noted in Aït-Sahalia, Mykland, and Zhang (2006), *bounce-back* data errors are caused by extreme round trips of recorded prices to unreasonably different price levels. If returns are immediately followed by a return with opposite signs and similar magnitudes and if their magnitudes are significantly different from those without the bounce-back effect, they are removed. For transactions that happen at the same time, we take the first transaction price recorded in the database. Because trading on the New York Stock Exchange is

interrupted overnight (after 4:00 p.m. and before 9:30 a.m. on next days), one might see that instantaneous volatility is not observable for the overnight return and we should omit those data that are affected by the interruption. However, our initial analysis shows that overnight returns do not necessarily include jumps. In other words, there are many days with overnight returns that do not include any unusual jumps in high-frequency data, although if they appear, it is more likely to be in the morning. Hence, in this paper, we take a different view of overnight returns. We consider that those overnight returns with jumps should also be regarded as part of our evidence. Instead of removing all of them, we keep them and include them in our tests. If jumps in those returns are detected by our tests, we count them as jumps in this study.

5.2. Empirical results

For all the return series, we apply both our big-jump test and our small-jump test, forming a combination of the QQ test with the belief measure as discussed in Section 3. We set the threshold level for the truncated power variation as in our simulation in Section 4. Once we apply these two methods, we mark those individual returns detected in graphs. Finally, we calculate the daily time-varying intensities of big and small jumps. All the tests are based on a significance level of 5%. We explain in this subsection the detailed graphical results for the S&P 500 index return series and Citigroup stock return series. Complete graphical results for all other indices and stocks over the entire sample period are available upon request. Overall numerical results for all series are reported in Table 6.

Before we show the test results, we first show what can be realized if there is no Lévy jump in the market. Fig. 1 illustrates the results of our QQ test and big-jump test on simulated returns under the no-jump model. The solid line shows the QQ-plot of test statistics applied to simulated five minute returns. The 95% confidence bands for the QQ test is plotted with dot-dashed lines.

We add in the same panel the thresholds for the big-jump test with dotted lines. As can be seen, if there is no jump, the solid line never leaves the envelope with dot-dashed lines.

Next we present the results for the S&P 500 index. Fig. 2 illustrates the results of our QQ test and our big-jump test. As in Fig. 1, we show the 95% confidence bands for the QQ test in dot-dashed lines and the thresholds for the big-jump test in dotted lines, along with the QQ-plot (in the solid line) of realized test statistics. As long as our test statistic is outside of the dot-dashed envelope, we can conclude that there is significant evidence of Lévy jumps. Notice that the solid QQ-plot not only leaves the dot-dashed envelope but also goes beyond the dotted line. This evidence of Lévy jumps is consistent with Li, Wells, and Yu (2008), who investigate their presence using a Baysian Markov Chain Monte Carlo method for the U.S. market index.

If evidence of Lévy jumps is found by our QQ test, we find small-jump arrivals with a reasonably high belief. To do this, we calculate the belief measure and present them in Fig. 3 (upper panel). We can flag small jumps based on this belief measure. We use 95% as a cutoff for the belief measure and detect small-jump arrivals. We also study the timing and intensities of small and big jumps for a better understanding of their dynamics. In the graph of the S&P 500 return series in Fig. 3 (lower panel), we put dots in circles for the returns flagged by our big-jump test. All the jumps detected by our belief measure are shown in the same panel with circles.

We count the number of jumps detected by our tests over the entire sample period and report them in both numbers and percentages in Table 6. We find evidence of both small and big jumps. Table 6 also presents 95% confidence bands used for both the big-jump and small-jump tests. To understand their dynamics, we also plot the time-varying daily intensities of jumps over time and show the graphs in the upper and lower panels, respectively, of Fig. 4. The graph of big jumps is the smoothed daily count of big jumps detected by the big-jump test. The graph of small jumps is

the smoothed daily expected number of jumps, where the expected number of jumps is obtained by adding up the values of our belief measure $b(t_i)$ for all returns within a day. Understanding the different dynamics of big and small Lévy jumps can be useful to incorporate in developing models for different types of risks in the index. We also find similar evidence for the Dow Jones Industrial Average.

We apply the same analysis on Citigroup stock returns and present the graphical results in Figs. 5, 6, and 7. Fig. 5 shows that the solid line for the QQ-plot of the test statistic applied to Citigroup stock returns leaves the 95% confidence bands from the envelope (dot-dashed lines) as well as the thresholds of our big-jump test (dotted lines). Hence, we conclude that there is evidence of Lévy jumps in these stock returns, too. We also calculate the belief measure. We plot the measure in the upper panel of Fig. 6 and present in the lower panel the detected jumps marked with dots and circles as we did for the S&P 500 index. This can become auxiliary data for setting up new dynamic models for small and big jumps in Citigroup equity prices. As mentioned earlier, we apply the same analysis and find qualitatively identical results for other individual stocks listed in Table 6. Their numerical results can be found therein.

There is an interesting systematic departure from the null distribution as evidenced by bumps in the belief measures at zero in Figs. 3 and 6 (upper panels). In both figures, there is an overabundance of test statistics around zero. We theorize that this is due to the tick size or to other microstructure noise remaining in five-minute returns. We stress that this departure from the diffusion model would not be detectable by competing tests, showing the versatility of our test. This also presents the possibility that our newly developed belief measure could be used in distinguishing jumps in equilibrium prices and market microstructure noise.

5.3. Comparison of evidence in S&P index and individual stock prices

We can compare the results for the S&P 500 index and Citigroup equity by looking at Figs 2 and 5. We see more deviation of the solid line from the dot-dashed lines signifying more Lévy jumps in Citigroup stock prices than in the S&P 500 index. This evidence also shows up in the comparison of return series figures with dots and circles in the lower panels of Figs 3 and 6. We have many more dots and circles for Citigroup equity prices than for the S&P 500 index. We can also compare Figs 4 and 7 and again see that the individual stock has more big and small jumps than the index.

We report in Table 6 the numbers of jumps detected in all series under consideration and the 95% confidence bands for both the small-jump and big-jump tests. From this table, we can explicitly compare the numbers of jumps for the indices and stocks. On average, we find that 0.50% and 0.32% of returns from the overall market indices during the sample period are detected by our small-jump and big-jump tests, respectively. Among individual stock returns, on average, we find that 0.78% and 0.41% are detected by our small-jump and big-jump tests, respectively. All the evidence for small jumps are based on a belief measure greater than 95%, which means that 5% of rejected returns could be due to random fluctuations of diffusion. We also repeat the same analysis using the significance level $\tilde{\alpha} = 1\%$, and the outcomes are similar to our earlier results with the level $\tilde{\alpha} = 5\%$. This significant evidence of small jumps suggests that stochastic volatility and Poisson-type jump models are not sufficient to capture the return dynamics in either U.S. market indices or individual equity prices. We expect the impact of small jumps to be a bit stronger in individual equities because more Lévy jumps are detected.

6. Concluding remarks

Given the extensive use of Lévy jump processes for continuous-time asset-pricing models, we introduce empirical methods to detect the presence and dynamics of small jumps as well as big jumps in financial markets, using discrete observations. In particular, we propose an indirect way to detect arrivals of small jumps using a combination of the QQ test and a belief measure, allowing us to control for false detection. We also suggest how to detect big jumps and the decomposition of jump risks. We apply our new tests on U.S. stock indices and individual stocks and find evidence that both types of return series would require incorporating Lévy-type jumps in pricing models in order to better capture their return dynamics. Indices and individual stocks tend to have different dynamics of Lévy jumps, leading us to conclude that incorporating separate models for the two different types of jump risk would improve financial management.

We suggest using high-frequency observations for our tests. With tick-by-tick transaction prices, the presence of microstructure noise could influence econometric inference on the underlying equilibrium prices. Depending on the structure and magnitude of noise, our test will be affected differently. However, if we choose the frequency of observations appropriately with the help of our belief measure, we do not expect the impact of noise to be serious in detecting jumps under our consideration. Though detailed analysis on the presence of noise is an interesting question, it is beyond the scope of the current article. We are currently investigating this issue.

Finally, we consider only U.S. large individual firms and overall market indices in our empirical study. It would be interesting to discover evidence of different types of risks embedded in stocks with different characteristics or other types of securities and investigate their implications for relevant financial applications.

36

Table 6: **Lévy jump intensity and 95% confidence bands for both tests**[†]

| Name	# of tests	# of big jumps	# of small jumps	big jump band	small jump band
		U.S. market indices			
Dow Jones	89,446	285 (0.32%)	460 (0.51%)	(-5.0139, 5.0139)	(-4.1973, 4.0963)
S&P 500	90,047	286 (0.32%)	442 (0.49%)	(-5.0238, 5.0238)	(-4.2088, 4.1666)
Average	89,747	285 (0.32%)	451 (0.50%)	(-5.0188, 5.0188)	(-4.2030, 4.1315)
		U.S. individual equities			
Alcoa	96,145	433 (0.45%)	842 (0.88%)	(-5.0362, 5.0362)	(-3.9772, 3.9575)
American International Group	96,361	387 (0.40%)	713 (0.74%)	(-5.0366, 5.0366)	(-4.0368, 4.0386)
American Express	96,423	366 (0.38%)	733 (0.76%)	(-5.0367, 5.0367)	(-4.0142, 3.9745)
Boeing	96,399	351 (0.36%)	763 (0.79%)	(-5.0367, 5.0367)	(-3.9932, 3.9173)
Citigroup	96,554	392 (0.40%)	719 (0.75%)	(-5.0370, 5.0370)	(-4.0188, 3.9782)
Caterpillar	96,099	354 (0.37%)	581 (0.60%)	(-5.0361, 5.0361)	(-4.2929, 4.2198)
DuPont	96,341	346 (0.36%)	692 (0.72%)	(-5.0366, 5.0366)	(-3.8974, 4.0340)
Walt Disney	96,546	399 (0.41%)	768 (0.80%)	(-5.0369, 5.0369)	(-3.9752, 3.9974)
General Electric	96,510	366 (0.38%)	610 (0.63%)	(-5.0369, 5.0369)	(-4.0773, 4.1338)
General Motors	96,321	535 (0.56%)	1039 (1.08%)	(-5.0365, 5.0365)	(-3.9175, 3.9173)
Home Depot	96,397	403 (0.42%)	823 (0.85%)	(-5.0367, 5.0367)	(-3.9329, 3.9910)
Honeywell	96,138	442 (0.46%)	858 (0.89%)	(-5.0362, 5.0362)	(-3.9541, 4.0135)
International Business Machine	96,707	387 (0.40%)	677 (0.70%)	(-5.0373, 5.0373)	(-4.0955, 4.0565)
Johnson & Johnson	96,420	394 (0.41%)	693 (0.71%)	(-5.0367, 5.0367)	(-4.0982, 4.0794)
J.P.Morgan Chase	96,463	409 (0.42%)	827 (0.86%)	(-5.0368, 5.0368)	(-3.9179, 3.9937)
Coca Cola	96,219	291 (0.30%)	614 (0.63%)	(-5.0363, 5.0363)	(-3.9937, 4.0345)
McDonald's	96,327	436 (0.45%)	859 (0.89%)	(-5.0366, 5.0366)	(-3.9666, 3.9585)
3M	96,139	318 (0.33%)	610 (0.63%)	(-5.0362, 5.0362)	(-4.0714, 4.0385)
Altria Group	96,326	462 (0.48%)	819 (0.85%)	(-5.0365, 5.0365)	(-4.0391, 4.0157)
Merck	96,283	476 (0.49%)	887 (0.92%)	(-5.0365, 5.0365)	(-3.9303, 3.9581)
Pfizer	96,452	446 (0.46%)	785 (0.81%)	(-5.0368, 5.0368)	(-4.0116, 3.9958)
Procter & Gamble	96,437	302 (0.31%)	578 (0.60%)	(-5.0367, 5.0367)	(-4.0174, 4.0922)
AT&T	94,862	490 (0.52%)	906 (0.96%)	(-5.0336, 5.0336)	(-3.9126, 3.9944)
United Technologies	96,153	347 (0.36%)	656 (0.68%)	(-5.0362, 5.0362)	(-4.0850, 4.0379)
Verizon	96,313	429 (0.45%)	853 (0.89%)	(-5.0365, 5.0365)	(-3.9167, 3.9780)
Walmart	96,380	320 (0.33%)	614 (0.64%)	(-5.0367, 5.0367)	(-4.0705, 4.0152)
Exxon Mobil	94,561	323 (0.34%)	579 (0.61%)	(-5.0330, 5.0330)	(-4.0640, 4.0559)
Average	96,232	398 (0.41%)	756 (0.78%)	(-5.0364, 5.0364)	(-4.0057, 4.0162)

[†] This table reports detailed results of our big-jump and small-jump tests, using five-minute log returns of U.S. market indices and individual equities over a five-year horizon from January 1, 2002 to December 31, 2006. Individual equities presented are component stocks of the Dow Jones Industrial Average, traded on the New York Stock Exchange. The component stocks traded on Nasdaq are excluded to maintain consistent trading mechanisms across different securities for comparison purposes. Hewlett-Packard is also excluded because of a significant missing data problem in the TAQ database. # of tests denotes the total number of observed test statistics during our sample period. # of big and small jumps denotes the numbers of jumps detected by our big-jump and small-jump tests, respectively. The big-jump and small-jump intensities (the rates of occurrence) are calculated based on the numbers of jumps detected by our big-jump and small-jump tests relative to the total numbers of tests and presented in parentheses next to the actual counts. Big-jump and small-jump bands are observed detection regions according to our big-jump detection rule and small-jump test using the belief measure as discussed in Section 3. We detect small (big) jumps if the observed test statistic at testing time t_i is outside of the small (big) jump band shown in this table.

Figure 1: **Graphical results of our jump tests in the absence of jumps**
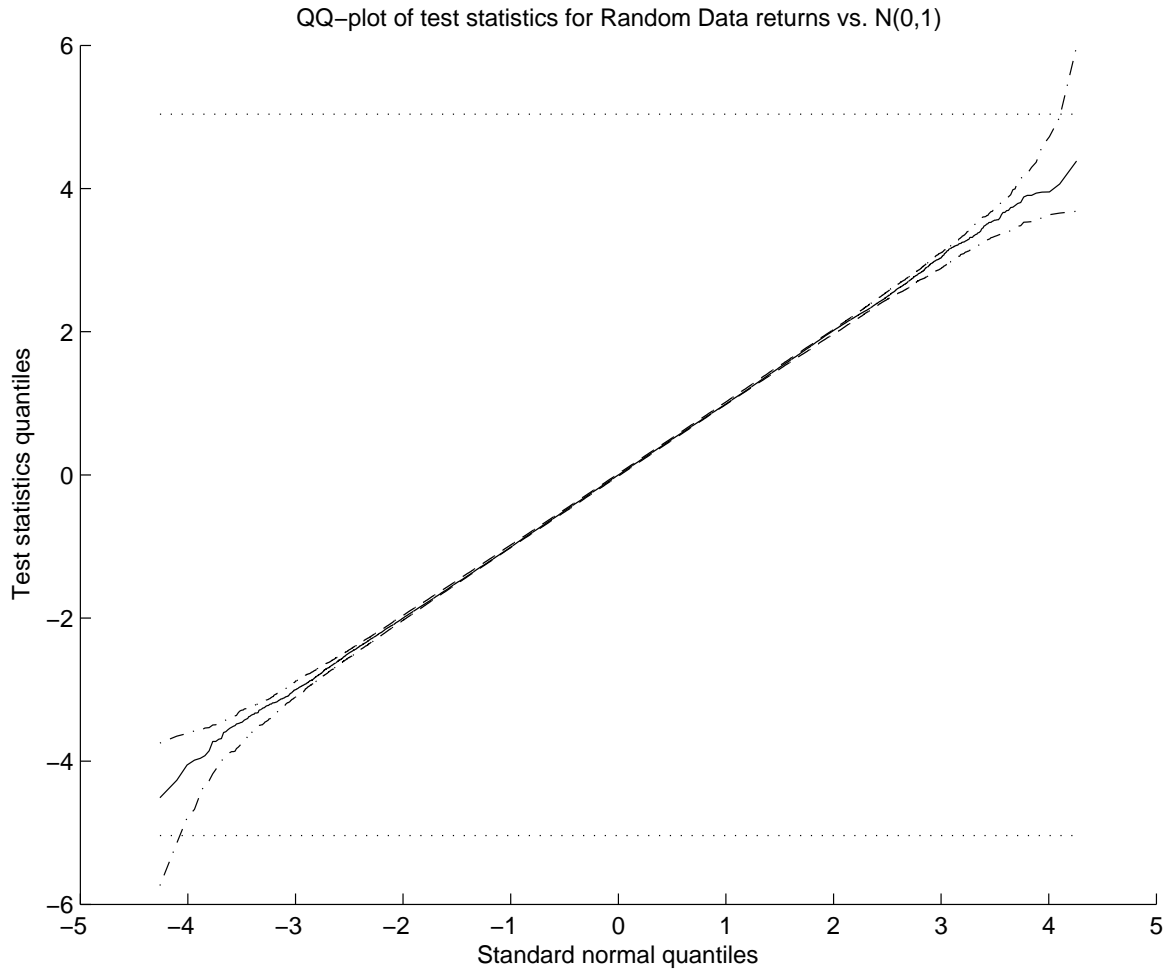
QQ–plot of test statistics for Random Data returns vs. N(0,1)

This graph illustrates the results of our QQ test and big-jump test on simulated returns under the no-jump model to compare empirical results using real data. The solid line shows the QQ-plot of realized test statistics, applied to simulated five-minute returns. The 95% confidence band for our QQ test is plotted with dot-dashed lines. The thresholds for our big-jump test are drawn with dotted lines. The time series of five-minute log returns are calculated by taking the first differences of log prices simulated from the diffusion process. The significance levels are 5%.

Figure 2: **Detecting Lévy jumps in the S&P 500 index**

QQ–plot of test statistics for S & P 500 returns vs. N(0,1)
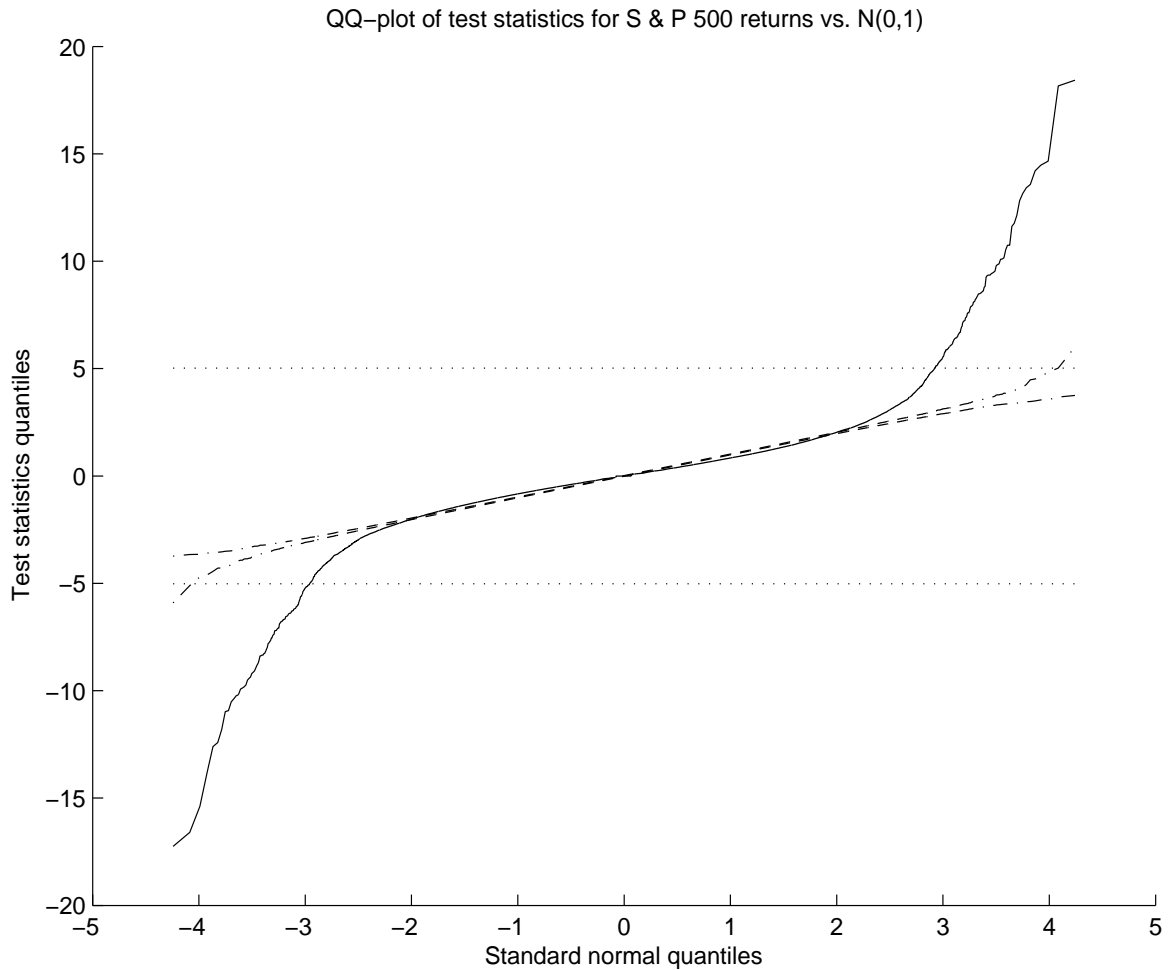
This graph illustrates the results of our QQ test and big-jump test on S&P 500 index returns during January 1, 2002 to December 31, 2006. The solid line shows the QQ-plot of realized test statistics applied to the time series of five-minute returns. Returns are calculated by the first differences of log S&P 500 index prices transacted on the New York Stock Exchange (NYSE). The 95% confidence band for our QQ test is plotted with dot-dashed lines. The thresholds of our big-jump test are drawn with dotted lines. The significance levels are 5%. Similar graphs applied to the Dow Jones Industrial Average are available upon request.

39

Figure 3: **Likelihood of Lévy jumps and detected jumps in the S&P 500 index**
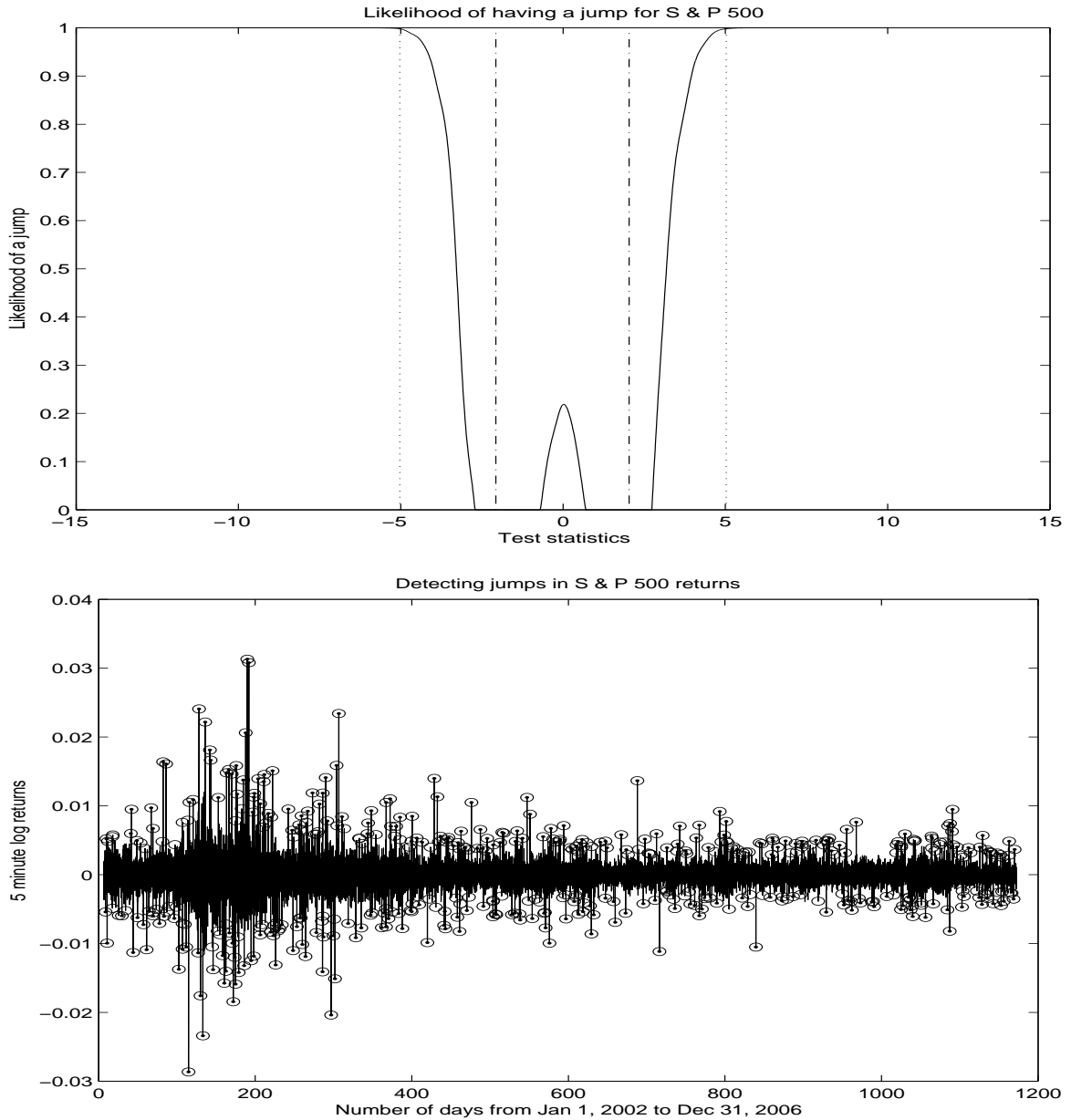
The graph in the upper panel shows the same dot-dashed lines for our QQ test and dotted lines for the thresholds of our big-jump test as shown in Fig. 2, and the likelihood of small jumps in solid lines. The graph in the lower panel shows the return series with dots in circles for jumps detected by our big-jump test and with circles for jumps detected by our small-jump test. Small jumps are after taking into account false jump detection by the likelihood of small jumps shown in the upper panel. Both significance levels and the false detection rate are 5%. Both panels are generated using the time series of five-minute log returns, calculated by taking the first differences of log S&P 500 index prices transacted on the New York Stock Exchange (NYSE) during January 1, 2002 to December 31, 2006. Similar graphs applied to the Dow Jones Industrial Average are available upon request.

Figure 4: **Realized time-varying intensities of Lévy jumps in the S&P 500**
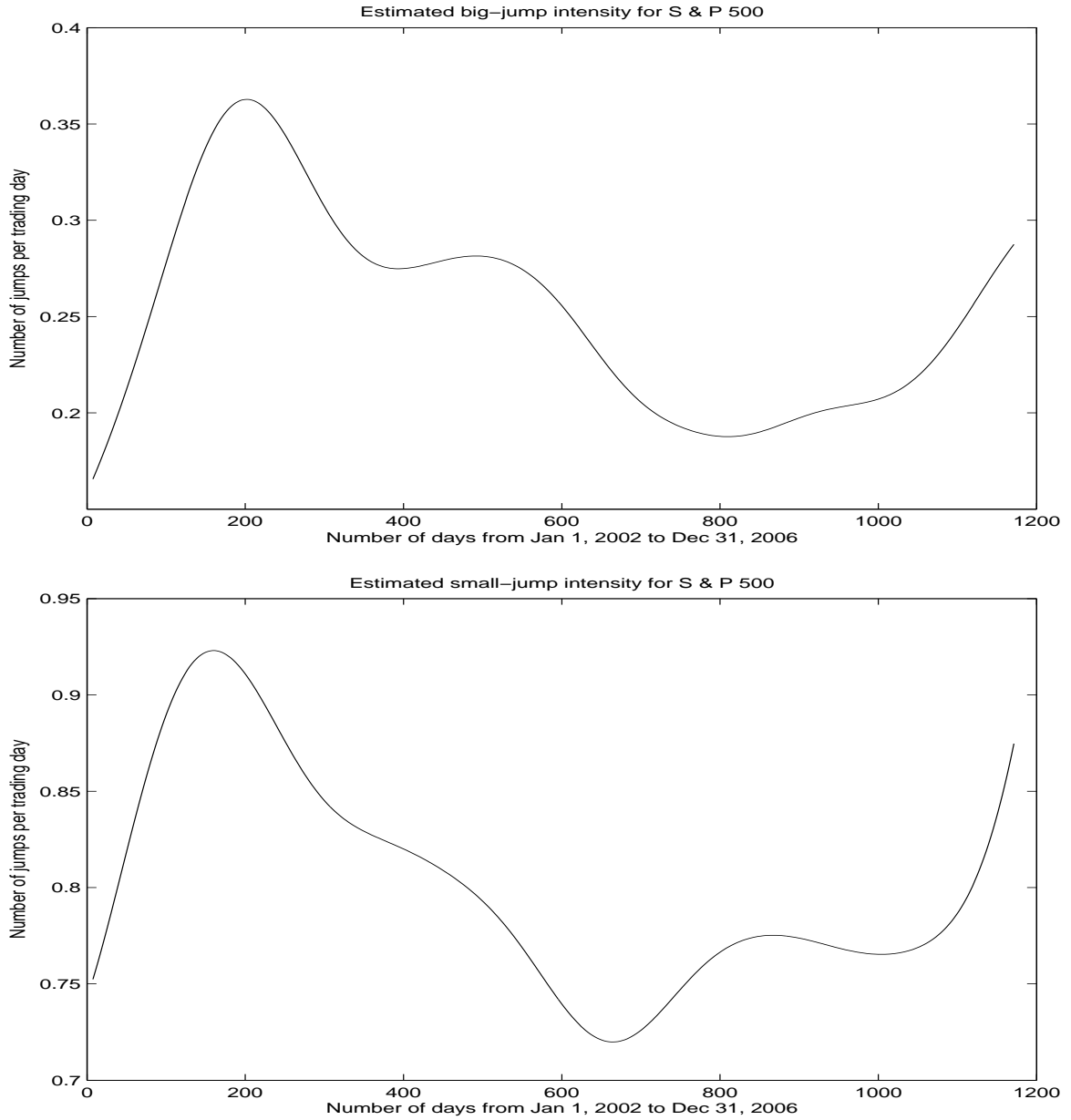
The graphs in the upper and lower panel show the jump intensities based on the number of jumps detected by our big-jump and small-jump tests. Small jumps are after discounting the jump counts by the value of their likelihood. The significance levels are 5%. Both figures are generated using the time series of five-minute log returns, calculated by taking the first differences of log S&P 500 index prices transacted on the New York Stock Exchange (NYSE) during January 1, 2002 to December 31, 2006. Similar graphs applied to the Dow Jones Industrial Average are available upon request.

Figure 5: **Detecting Lévy jumps in Citigroup**

QQ–plot of test statistics for Citigroup returns vs. N(0,1)
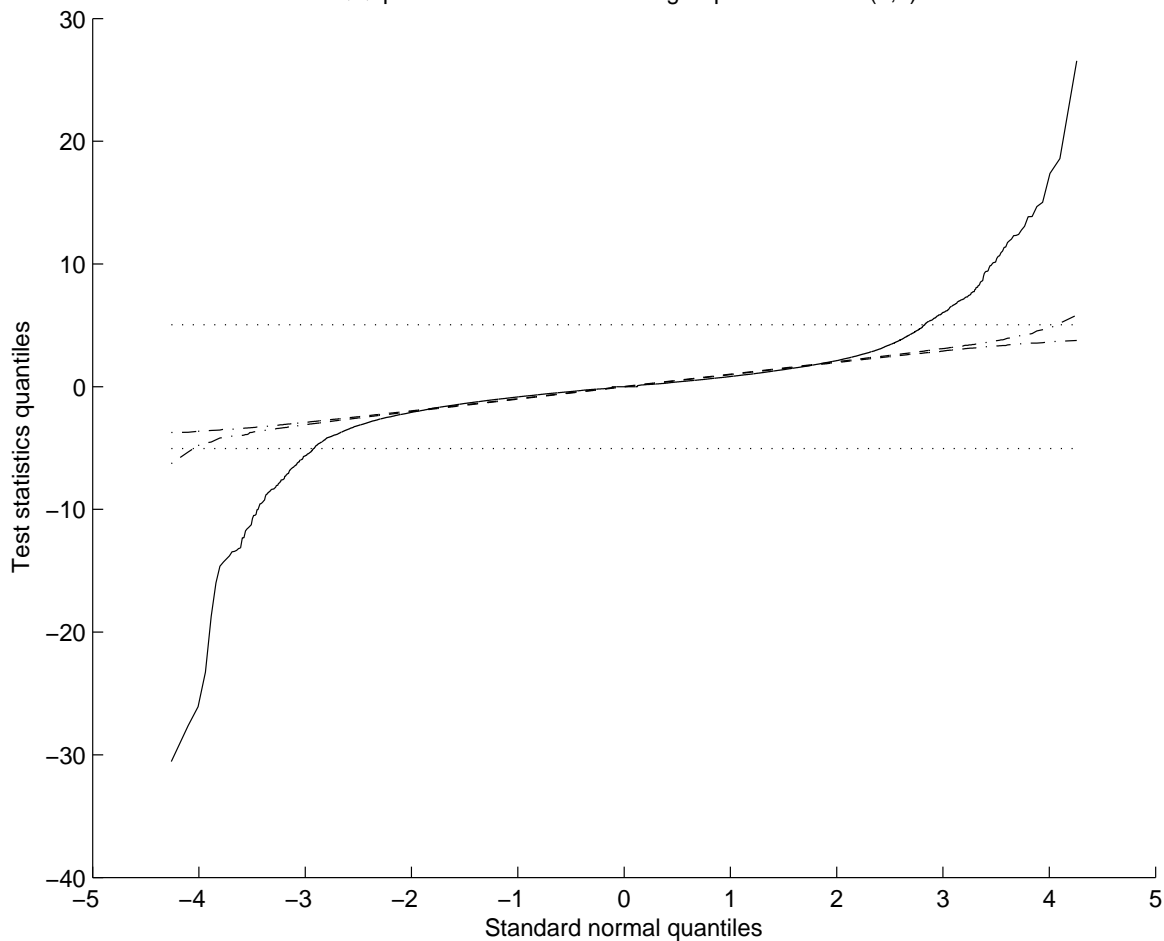
This graph illustrates the results of our QQ test and big-jump test on Citigroup returns during January 1, 2002 to December 31, 2006. The solid line shows the QQ-plot of realized test statistics applied to a time series of five-minute returns. Returns are calculated by the first differences of log Citigroup stock prices transacted on the New York Stock Exchange (NYSE). The 95% confidence band for our QQ test is plotted with dot-dashed lines. The thresholds of our big-jump test are drawn with dotted lines. The significance levels are 5%. Similar graphs applied to all the other individual stocks listed in Table 6 are available upon request.

Figure 6: **Likelihood of Lévy jumps and detected jumps in Citigroup**
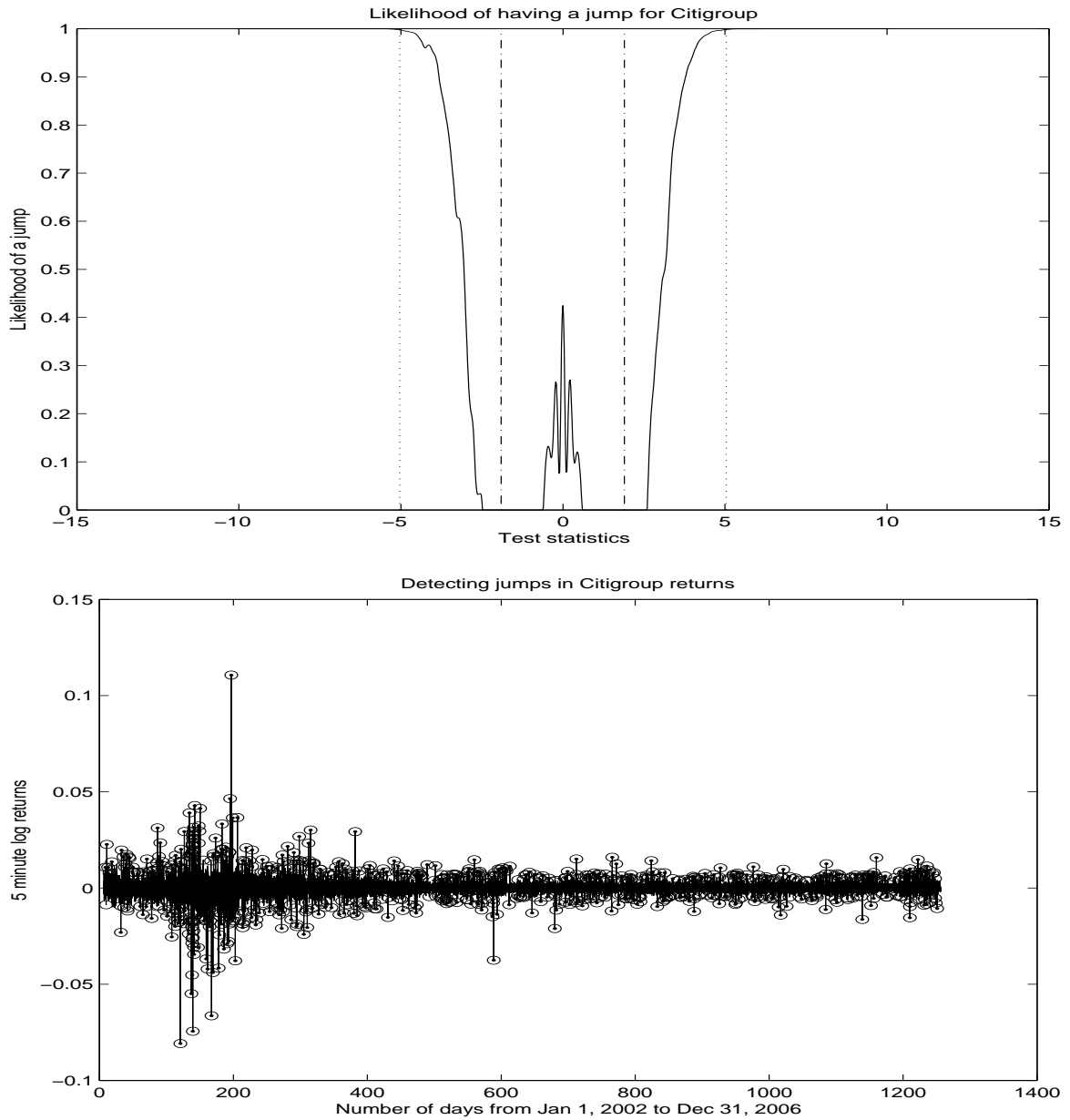
The graph in the upper panel shows the same dot-dashed lines for our QQ test and dotted lines for the thresholds of our big-jump test as shown in Fig. 5 and the likelihood of small jumps in solid lines. The graph in the lower panel shows the return series with dots in circles for jumps detected by our big-jump test and with circles for jumps detected by our small-jump test. Small jumps are after taking into account false jump detection by the likelihood of small jumps shown in the upper panel. Both significance levels and false detection rate are 5%. Both figures are generated using the time series of five-minute log returns, calculated by taking the first differences of log Citigroup stock prices transacted on the New York Stock Exchange (NYSE) during January 1, 2002 to December 31, 2006. Similar graphs applied to all the other individual stocks listed in Table 6 are available upon request.

43

Figure 7: **Realized time-varying intensities of Lévy jumps in Citigroup**
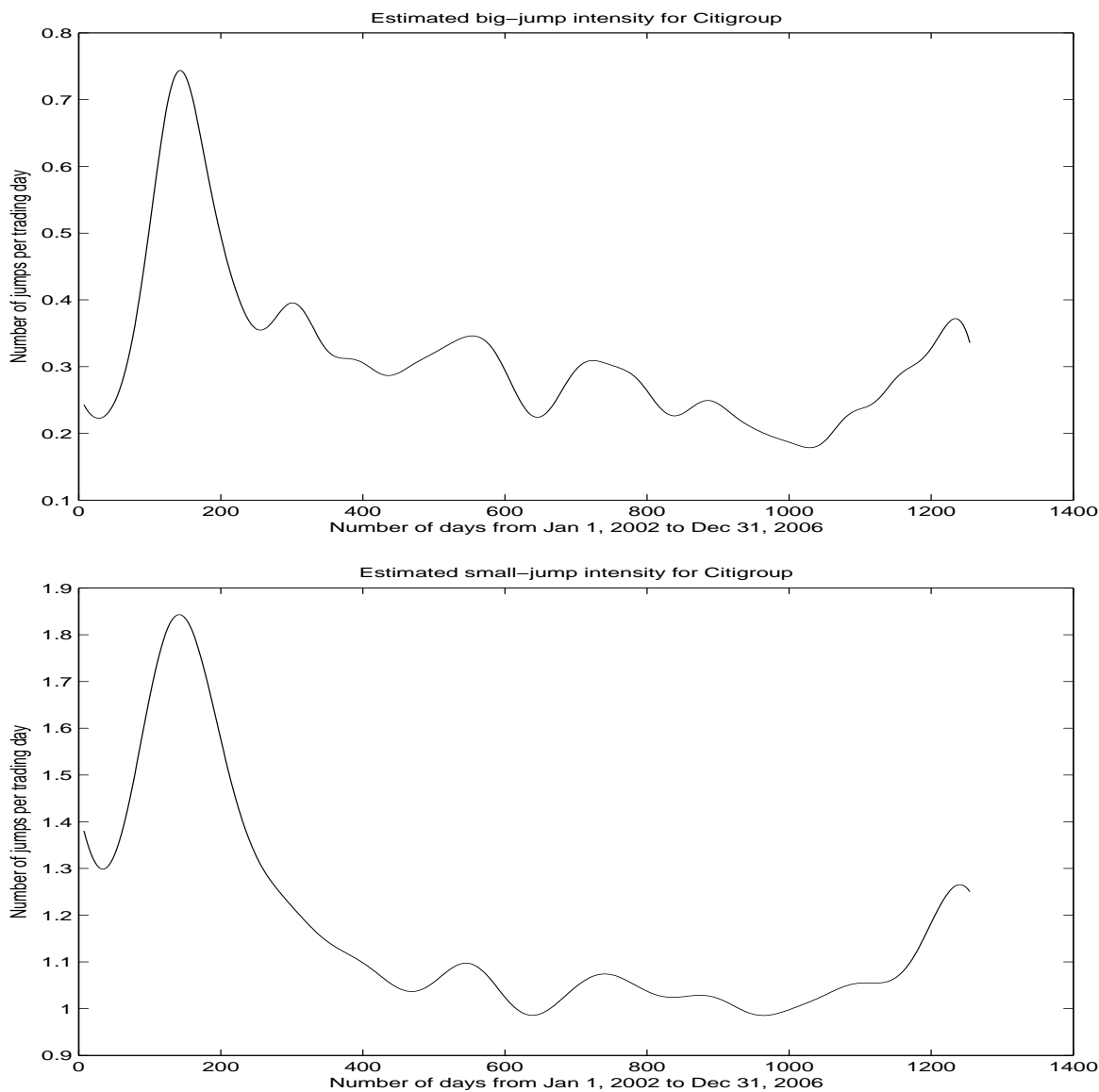
The graphs in the upper and lower panel show the jump intensities based on the number of jumps detected by our big-jump and small-jump tests, respectively. Small jumps are after discounting the jump counts by the value of their likelihood. The significance levels are 5%. Both figures are generated using the time series of five-minute log returns, calculated by taking the first differences of log Citigroup stock prices transacted on the New York Stock Exchange (NYSE) during January 1, 2002 to December 31, 2006. Similar graphs applied to all the other stocks listed in Table 6 are available upon request.

Appendix

A.1. Assumption 1

Mathematically, Assumption 1 can be written as follows. For any $\epsilon > 0$,

$$\textbf{A1.1} \quad \sup_i \sup_{t_i \leq u \leq t_{i+1}} |\mu(u) - \mu(t_i)| = O_p(\Delta t^{\frac{1}{2}-\epsilon}) \tag{18}$$

$$\textbf{A1.2} \quad \sup_i \sup_{t_i \leq u \leq t_{i+1}} |\log \sigma(u) - \log \sigma(t_i)| = O_p(\Delta t^{\frac{1}{2}-\epsilon}). \tag{19}$$

We use O_p notation in this study to mean that, for random vectors $\{X_n\}$ and a nonnegative random variable $\{d_n\}$, $X_n = O_p(d_n)$, if there exists a finite constant M_δ such that $P(|X_n| > M_\delta d_n) < \delta$ for each $\delta > 0$, eventually.

A.2. Proof of Proposition 1

Conditional on $\tau > r$, we define the process $\bar{S}(t) = S(t + \tau - r)$. Since τ is independent of S, this process still satisfies (2), assumptions A1.1 and A1.2, and $\bar{S}(r) = S(\tau)$. Thus, without loss of generality, we can assume that τ is a non-random time.

Since there are only a finite number of jumps of absolute size greater than one on finite intervals, such jumps will not eventually be included in the computation of $\widehat{\sigma(t)}$ almost surely. Thus, we can assume without loss of generality that the Lévy measure of the process $L(t)$ is concentrated on $[-1, 1]$. Denote the log return process of the standard model (1) by $dX(t) = \mu(t)dt + \sigma(t)dW(t)$ and denote the increments of this process as $b_i = X(t_i) - X(t_{i-1})$, and the increments of the Lévy process as $c_i = L(t_i) - L(t_{i-1})$. The sequence $a = b + c$ then forms the increments of the logarithm of the full Lévy model (2) used in the calculation of $\widehat{\sigma(\tau)}$ in (4).

In the case of truncated power variation, we note that for $d = g\Delta t^{\widetilde{\omega}}$ with $0 < \widetilde{\omega} < 1/2$,

$$\sum_{i=1}^{K}(b_i + c_i)^2 I_{\{|b_i| \leq d/2\}} I_{\{|c_i| \leq d/2\}} \leq \sum_{i=1}^{K} a_i^2 I_{\{|a_i| \leq d\}} \leq \sum_{i=1}^{K} \left(b_i + c_i I_{\{|c_i| \leq 2d\}}\right)^2. \tag{20}$$

45

It is well known that for a model without jump, both

$$\frac{\Delta t^{-1}}{K} \sum_{i=1}^{K} b_i^2 \xrightarrow{P} \sigma^2(\tau) \qquad \text{and} \qquad \frac{\Delta t^{-1}}{K} \sum_{i=1}^{K} b_i^2 I_{\{|b_i|\leq d/2\}} \xrightarrow{P} \sigma^2(\tau)$$

estimate the instantaneous volatility consistently as $\Delta t \to 0$. To prove our theorem, we will need to show that the remaining terms go to zero in probability. First note that by a simple direct calculation (see also Jacod, 2005),

$$\frac{\Delta t^{-1}}{K} \sum_{i=1}^{K} c_i^2 I_{\{|c_i|\leq 2d\}} \xrightarrow{P} 0.$$

Then, by the Cauchy-Schwartz inequality, we have

$$\sum_{i=1}^{K} b_i c_i I_{\{|c_i|\leq 2d\}} \leq \left(\sum_{i=1}^{K} b_i^2 \sum_{i=1}^{K} c_i^2 I_{\{|c_i|\leq 2d\}} \right)^{1/2}$$

and hence, the upper bound in (20) converges to $\sigma^2(\tau)$ in probability.

We now turn our attention to the lower bound in (20). Note that

$$|\sum_{i=1}^{K} b_i^2 I_{\{|b_i|\leq d/2\}} I_{\{|c_i|\leq d/2\}} - \sum_{i=1}^{K} b_i^2 I_{\{|b_i|\leq d/2\}}| \leq \left(\sum_{i=1}^{K} b_i^4 I_{\{|b_i|\leq d/2\}} \sum_{i=1}^{K} (1 - I_{\{|c_i|\leq d/2\}})^2 \right)^{1/2}.$$

However,

$$E \frac{1}{K} \sum_{i=1}^{K} (1 - I_{\{|c_i|\leq d/2\}})^2 = P(|c_i| > d/2) \to 0,$$

as $\Delta t \to 0$ (see, e.g., Barndorff-Nielsen, Shephard, and Winkel, 2006). Thus, since the truncated power variation of the model without jumps is known to be bounded in probability, we have

$$\frac{\Delta t^{-1}}{K} \sum_{i=1}^{K} b_i^2 I_{\{|b_i|\leq d/2\}} I_{\{|c_i|\leq d/2\}} \xrightarrow{P} \sigma^2(\tau).$$

All the remaining terms in the lower bound of (20) are bounded by their corresponding counterparts in the upper bound and therefore, they all go to zero. This concludes the proof.

A.3. Proof of Theorem 1

For simplicity of notation, let $t^+(t) = min\{t_i \geq t\}$ and $t^-(t) = \max\{t_i < t\}$. Note that $t^+(t) - t^-(t) = \Delta t$, $t^+(t) \to t$, and $t^-(t) \to t$ as $\Delta t \to 0$. Since $L(t)$ does not contain any Gaussian component and $\Delta L(\tau) = 0$ almost surely, a simple calculation using characteristic functions shows $L(\tau^+(t)) - L(\tau^-(t)) \xrightarrow{P} 0$ as $\Delta t \to 0$ (see, e.g., Bertoin, 1998, Proposition I.2). Therefore,

$$\frac{\log S(t^+(t))/S(t^-(t))}{\Delta t^{1/2}} \xrightarrow{\mathcal{D}} N(0, \sigma^2(t)).$$

The first statement of the theorem now follows by Slutsky's lemma and Proposition 1.

For a fixed $h > 0$, there is a decomposition $L(t) = L_1(t) + L_2(t)$ such that $\Delta L_1 \leq h$, L_2 is a compound Poisson process with jumps of size greater than h and with L_1 and L_2 independent. The jump times of L_2 coincide with $\tau_{k,h}$ by definition. Since L_1 and L_2 are independent, we have $L_1(t^+(\tau_{k,h})) - L_1(t^-(\tau_{k,h})) \xrightarrow{P} 0$ and $P(\log S(t^+(\tau_{k,h}))/S(t^-(\tau_{k,h})) \geq h) \to 1$ for all k. Since L_2 has only a finite number of jumps on $(0, T)$ almost surely, we see that the definition of the estimator of volatility implies $\widehat{\sigma(\tau_{h,k})} \to \sigma(\tau_{h,k})$ and (8) follows by Slutsky's lemma and simple algebra.

References

Aït-Sahalia, Y., 2002. Telling from discrete data whether the underlying continuous-time model is a diffusion. Journal of Finance 57, 2075–2112.

Aït-Sahalia, Y., 2004. Disentangling diffusion from jumps. Journal of Financial Economics 74, 487–528.

Aït-Sahalia, Y., Jacod, J., 2008. Fisher's information for discretely sampled Lévy processes. Econometrica 76, 727–761.

Aït-Sahalia, Y., Jacod, J., 2009a. Estimating the degree of activity of jumps in high frequency data. Annals of Statistics 37, 2202–2244.

Aït-Sahalia, Y., Jacod, J., 2009b. Testing for jumps in a discretely observed process. Annals of Statistics 37, 184–222.

Aït-Sahalia, Y., Mykland, P. A., Zhang, L., 2006. Ultra high frequency volatility estimation with dependent microstructure noise. Journal of Econometrics, forthcoming.

Andersen, T. G., Benzoni, L., Lund, J., 2002. An empirical investigation of continuous-time equity return models. Journal of Finance 57, 1239–1284.

Andersen, T. G., Bollerslev, T., Diebold, F., Ebens, H., 2001. The distribution of realized stock return volatility. Journal of Financial Economics 61, 43–76.

Bakshi, G., Cao, C., Chen, Z., 1997. Empirical performance of alternative option pricing models. Journal of Finance 52, 2003–2049.

Bakshi, G., Carr, P., Wu, L., 2008. Stochastic risk premiums, stochatic skewness in currency options, and stochastic discount factors in international economies. Journal of Financial Economics 87, 132–156.

Bakshi, G. S., Ju, N., Ou-Yang, H., 2006. Estimation of continuous-time models with an application to equity volatility. Journal of Financial Economics 82, 227–249.

Barndorff-Nielsen, O. E., Shephard, N., Winkel, M., 2006. Limit theorems for multipower variation in the presence of jumps. Stochastic Processes and Their Applications 116, 796–806.

Bertoin, J., 1998. Lévy Processes. Cambridge: Cambridge University Press.

Bollerslev, T., Law, T. H., Tauchen, G., 2008. Risk, jumps, and diversification. Journal of Econometrics 144, 234–256.

Carr, P., Geman, H., Madan, D. B., Yor, M., 2002. The fine structure of asset returns: An empirical investigation. Journal of Business 75, 305–332.

Carr, P., Madan, D. B., 1998. Option valuation using the fast Fourier transform. Journal of Computational Finance 2, 61–73.

Carr, P., Wu, L., 2003. What type of process underlies options? A simple robust test. Journal of Finance 58, 2581–2610.

Carr, P., Wu, L., 2004. Time-changed Lévy processes and option pricing. Journal of Financial Economics 71, 113–141.

Carr, P., Wu, L., 2007. Stochastic skew in currency options. Journal of Financial Economics 86, 213–247.

Chambers, J., Mallows, C., Stuck, B., 1976. A method for simulating stable random variables. Journal of the American Statistical Association 71, 340–344.

Chernov, M., Gallant, A. R., Ghysels, E., Tauchen, G., 2003. Alternative models for stock price dynamics. Journal of Econometrics 116, 225–257.

Cox, J. T., Ingersoll, J. E., Ross, S. A., 1985. A theory of the term structure of interest rates. Econometrica 53, 385–407.

Duffie, D., Pan, J., Singleton, K., 2000. Transform analysis and asset pricing for affine jump diffusions. Econometrica 68, 1343–1376.

Eraker, B., Johannes, M., Polson, N., 2003. The impact of jumps in volatility and returns. Journal of Finance 53, 1269–1300.

Fan, J., Gijbels, I., 1996. Local Polynomial Modelling and Its Applications. London: Chapman & Hall.

Hernandez-Campos, F. ans Marron, J. S., Samorodnitsky, G., Smith, F. D., 2004. Variable heavy tails in internet traffic. Performance Evaluation 58, 261–284.

Heston, S., 1993. A closed-form solution for options with stochastic volatility with applications to bonds and currency options. Review of Financial Studies 6, 327–343.

Huang, J. Z., Wu, L., 2004. Specification analysis of option pricing models based on time-changed lévy processes. Journal of Finance 59, 1405–1439.

Huang, X., Tauchen, G., 2005. The relative contribution of jumps to total price variance. Journal of Financial Econometrics 3, 456–499.

Jacod, J., 2005. Asymptotic properties of power variations of lévy processes. ESAIM: Probability and Statistics 11, 173–196.

Johannes, M., 2004. The statistical and economic role of jumps in interest rates. Journal of Finance 59,

227–260.

Kloeden, P. E., Platen, E., 1992. Numerical Solution of Stochastic Differential Equations. Springer-Verlag.

Lee, S., Mykland, P. A., 2008. Jumps in financial markets: A new nonparametric test and jump dynamics. Review of Financial Studies 21, 2535–2563.

Li, H., Wells, M. T., Yu, C. L., 2008. A bayesian analysis of return dynamics with lévy jumps. Review of Financial Studies 21, 2345–2378.

Mancini, C., 2006. Estimating the integrated volatility in stochastic volatility models with lévy type jumps. Working paper, University of Florence.

Merton, R. C., 1976. Option pricing when underlying stock returns are discontinuous. Journal of Financial Economics 3, 125–144.

Pan, J., 2002. The jump-risk premia implicit in options: Evidence from an integrated time-series study. Journal of Financial Economics 63, 3–50.

Piazzesi, M., 2003. Bond yields and the federal reserve. Journal of Political Economy 113, 311–344.

Ruppert, D., Sheather, S., Wand, M., 1995. An effective bandwidth selector for local least squares regression. Journal of the American Statistical Association 90, 1257–1270.

Todorov, V., Tauchen, G., 2008. Activity signature plots and the generalized blumenthal-getoor index. Working paper, Duke University and Northwestern University.